

Review

Low Platinum-Content Electrocatalysts for Highly Sensitive Detection of Endogenously Released H₂O₂

Ana Morais ^{1,2}, Patrícia Rijo ^{1,3} , Belen Batanero ²  and Marisa Nicolai ^{1,*} 

¹ CBIOS—Universidade Lusófona's Research Centre for Biosciences & Health Technologies, Campo Grande 376, 1749-024 Lisbon, Portugal

² Department of Organic Chemistry & Inorganic Chemistry, University of Alcalá, 28805 Alcalá de Henares, Spain

³ iMed.Ulisboa—Research Institute for Medicines and Pharmaceutical Sciences, Faculty of Pharmacy, University of Lisbon, Av. Prof. Gama Pinto, 1649-003 Lisbon, Portugal

* Correspondence: marisa.nicolai@ulusofona.pt

Abstract: The commercial viability of electrochemical sensors requires high catalytic efficiency electrode materials. A sluggish reaction of the sensor's primary target species will require a high overpotential and, consequently, an excessive load of catalyst material to be used. Therefore, it is essential to understand nanocatalysts' fundamental structures and typical catalytic properties to choose the most efficient material according to the biosensor target species. Catalytic activities of Pt-based catalysts have been significantly improved over the decades. Thus, electrodes using platinum nanocatalysts have demonstrated high power densities, with Pt loading considerably reduced on the electrodes. The high surface-to-volume ratio, higher electron transfer rate, and the simple functionalisation process are the main reasons that transition metal NPs have gained much attention in constructing high-sensitivity sensors. This study has designed to describe and highlight the performances of the different Pt-based bimetallic nanoparticles and alloys as an enzyme-free catalytic material for the sensitive electrochemical detection of H₂O₂. The current analysis may provide a promising platform for the prospective construction of Pt-based electrodes and their affinity matrix.

Keywords: hydrogen peroxide; electrochemical sensing; cathodic reduction; platinum-based electrocatalysts; bimetallic alloys



Citation: Morais, A.; Rijo, P.; Batanero, B.; Nicolai, M. Low Platinum-Content Electrocatalysts for Highly Sensitive Detection of Endogenously Released H₂O₂.

Biosensors **2022**, *12*, 672. <https://doi.org/10.3390/bios12090672>

Received: 30 June 2022

Accepted: 12 August 2022

Published: 23 August 2022

Publisher's Note: MDPI stays neutral with regard to jurisdictional claims in published maps and institutional affiliations.



Copyright: © 2022 by the authors. Licensee MDPI, Basel, Switzerland. This article is an open access article distributed under the terms and conditions of the Creative Commons Attribution (CC BY) license (<https://creativecommons.org/licenses/by/4.0/>).

1. Introduction

As a natural metabolite commonly found in all aerobic organisms [1], accurate surveillance of hydrogen peroxide (H₂O₂) is of significant interest in biomedical research, given its physiological and pathological roles.

This paper proposes various Pt-based alloys and composites as suitable catalytic electrode layers for the accurate and sensitive detection of H₂O₂. These Pt-based alloys take advantage of the embedded secondary metal (for instance, transition metal) nanoparticles' synergistic effect and the increment of the effective area to enhance the sensing electrode's signal.

Hydrogen peroxide (H₂O₂) is an existing non-radical oxidant in virtually all aerobic organisms. As one of the simplest peroxides that vary according to the medium's pH, H₂O₂ can act as an oxidising or reducing agent [2]. Both redox reactions give rise to environmental-friendly side-reaction products, water or oxygen. Thus, for environmental reasons, H₂O₂ is preferred over other chemicals in most industrial applications.

H₂O₂ [3] is a covalent liquid, readily miscible with water, hence is a chemical compound that plays some pivotal roles in a wide range of industrial applications. These include the processing of petrochemicals (plastic industries) [4], paper-products manufacturing (pulp and paper bleaching) [5], textile industry [6], chemical industries [7], medical

diagnostics [8], cosmetics [9], and biological analysis and biochemistry [10]. In addition, H_2O_2 acts as an essential mediator in environmental analysis, pollution control [11], pharmaceutical industries (research and manufacturing), and clinical research [8].

Given the inherent antiseptic and antibacterial properties of H_2O_2 , it is also used as a cleaning product [12] and in food processing [13]. Therefore, H_2O_2 is commonly used as an antiseptic and sterilising agent in the food industry (e.g., sterilisation of aseptic packaging containers [14] to prolong products' shelf life). Therefore, it is involved in cold pasteurisation and milk preservation to slow down the growth of bacteria and delay the fermentation of products [15].

In addition, as a powerful oxidising agent, H_2O_2 is widely used in the mining process [16]; it aids in synthesising various organic compounds [17] and works as an oxidant for constructing liquid-based fuel cells [18]. It is also employed in treating contaminated soils and wastewater, given its enrolment in Fenton's reaction with the formation of the highly reactive hydroxyl radicals responsible for the aromatic and halogenated compounds' withdrawal [19,20].

Biochemically [3], H_2O_2 is a ubiquitous small molecule of living cells that arises during the incomplete reduction of molecular oxygen as a by-product of cellular metabolism. It is thereby an uncharged molecule, which results as a side-product from a wide range of biological processes. Namely from a broad spectrum of selective oxidases in the mitochondria, such as glucose oxidase (GOx), cholesterol oxidase (ChoOx), glutamate oxidase (GLOx), oxalate oxidase (OxaOx), lactate oxidase (LOx), urate oxidase (UOx), alcohol oxidase (ALOx), lysine oxidase (LyOx), D-amino acid oxidase (DAAO), and xanthine oxidase, among others. H_2O_2 can also result as a direct product of superoxide dismutation by the superoxide dismutase enzyme (SOD) [21].

Because H_2O_2 is a prominent mediator product of various redox reactions, it is possible to monitor and establish the concentration of other biological species involved, such as glucose, lactate, urate, and cholesterol [22], by measuring the level of H_2O_2 .

As a chemical substance, and given its relatively long lifetime at a physiological level, uncharged H_2O_2 can diffuse freely through phospholipid membranes, travelling within and between cells [23]. Therefore, H_2O_2 is allowed to enter other cell compartments' readily reaching its cellular targets, which might induce various biological damages when found at oxidative stress levels.

Because of its ability to react with ubiquitous transition metal ions, H_2O_2 can readily generate one of the most reactive ROS, through Fenton or Haber–Weiss reactions, the hydroxyl radicals (OH^\bullet) [24]. Above physiological levels, H_2O_2 can be potentially toxic in the body after reacting with ferrous (Fe^{2+}) or cuprous (Cu^+) ions, frequently attainable at the active structural sites of proteins. The hydroxyl radical can indifferently react with all found molecules (lipids, proteins, nucleic acids, and carbohydrates), oxidising them. As a result, OH^\bullet leads to severe oxidative damage in numerous molecules that comprise body tissues, with phospholipids, proteins, and DNA as the most targeted biomolecules in cell membranes [24].

Alongside the release of endogenous H_2O_2 , there is an antioxidant system composed of several enzymes that balance the oxidative species' concentration. Some enzymes designed to eliminate H_2O_2 at the cellular level, preventing its oxidative effects [25], are catalase, glutathione-peroxidases, and peroxiredoxins.

However, when there is a depletion of antioxidant species in the organism, an imbalance between the rate of the ROS endogenous production and the antioxidant mechanism that neutralises or repairs the resulting damage occurs [1].

For some time now, a significant amount of scientific evidence has pointed to oxidative stress's prominent role in many pathological conditions [1,26]. The excessive presence of multiple distinct ROS and reactive nitrogen (RNS) species among the biological fluids disrupts cellular redox homeostasis, of which H_2O_2 is the most widely representative. As a result, the accumulation of H_2O_2 is closely correlated with an increased risk of autoimmune [27], inflammatory [27], and angiocardipathic diseases [27], and likewise is

involved in the own ageing natural process [28], including the age-related neurodegeneration [29]. Therefore, H_2O_2 is an early indicator of ischemia/reperfusion injury [1], traumatic brain injury, neurodegenerative disorders, impaired learning and memory functions [28], atherosclerosis, myocardial infarction [27], diabetes, cancer [24,30], and related kidney injury diseases [31], and others.

Apart from the adverse effects stated above, in terms of the vital physiological functions of living organisms, H_2O_2 is an essential metabolite that, thanks to its free transit across cells, acts as a mediator in most cellular metabolic reactions [26]. Therefore, H_2O_2 is involved in many biological processes with a significant role at the cellular level of the human organism. Accordingly, it participates in the host-defence mechanism of the immune system and as a signalling molecule in the regulation of diverse biological processes such as the coordination of protein synthesis, immune-cells activation, vascular remodelling, and cell apoptosis.

In eukaryotes, particularly in higher vertebrates, endogenous H_2O_2 mediates several physiological processes [29]. It is therefore generated in precise locations close to the responsive signalling molecules. Additionally, H_2O_2 may be evenly produced by activating NADPH oxidases in target cells. Therefore, H_2O_2 act as a secondary messenger in multicellular organisms, emerging as a specific response to growth factors and cytokines in cell division, differentiation, and migration [32]. Hence, H_2O_2 is involved in modulation and signalling redox metabolism under physiological conditions as a signalling molecule. It regulates cell growth, proliferation, and differentiation and is further responsible for cellular migration.

As a second messenger, H_2O_2 triggers a series of specific oxidations (through the oxidative modulation of sensitive redox-proteins, also called redox switches), which activates the proteins' sequence downstream as the cell's metabolic response. Occurrence, which in turn enables cellular' proliferation, survival, or extinction.

The outcome depends on which downstream pathways have been activated: homeostatic, pathological, or protective. Hence, when at low physiological levels, H_2O_2 can also initiate protective responses to limit or repair cellular oxidative damage [1,33].

The disposal of metabolites, such as H_2O_2 , represents a metabolic mechanism that allows regulating their levels in the human body. Since the ubiquitous H_2O_2 is usually excreted through body fluids such as urine, tears, and sweat or in breathing during the regular functioning of the human body, the concentration of H_2O_2 found in those samples can be a valuable tool to assess the degree of oxidative stress on the human organism [10]. Therefore, H_2O_2 works as a biomarker, a parameter used to diagnose and survey various diseases.

2. Hydrogen Peroxide Electrochemical Detection

Within the sphere of development of biosensor technologies for medical applications aiming to surveil a myriad of disorders, the accurate quantification of metabolites involved in the most common persistent health conditions has increasingly attracted attention. Particularly H_2O_2 , due to its role as a metabolite implicated in a broad spectrum of different health disorders [31,34–36] and its central role as a regulator of various biological processes. As a result, a high-sensitive quantification of H_2O_2 is relevant for developing a reliable diagnosis of the different medical conditions in humans and, hence, subject to considerable research efforts of strict detection requirements.

2.1. H_2O_2 Sensing Analytical Methods

The scope of different analytical methods used in the determination of H_2O_2 has included the techniques: fluorimetry, spectrophotometry, fluorescence [37], chromatography [38], chemiluminescence [39], titrimetry [40], and electrochemistry [41]. However, most of these methods reveal some inherent technical drawbacks, such as low sensitivity and selectivity, long testing time, vulnerability to interferences, and complicated or expensive equipment. Among the existing techniques for H_2O_2 detection, the electrochemistry approach has proved to be the most attractive/efficient tool [41]. It allows for a short-

term accurate and selective evaluation of a low detection limit on low-cost instrumentation. Moreover, it is one of the most versatile methods because it holds a wide dynamic span, simple instrumentation, and easy miniaturisation, becoming suitable for quantifying changes in H_2O_2 levels in vivo in the brain [42]. Furthermore, electrochemical technology based on the catalytic activity allows for an H_2O_2 detection method of simple, fast, and cost-effective operation [43] once H_2O_2 is an electroactive molecule that can be oxidised or reduced on the surface of a solid electrode.

Nevertheless, the electrochemical processes might be constrained by the sluggish kinetics of the electrodes, and the high overpotential required [44], which will reduce the sensing performance. Consequently, the electrode's catalytic activity for H_2O_2 detection is crucial in the sensor/biosensor device's performance. Therefore, modification of the electrodes is an essential task for developing a reliable sensor/biosensor.

2.2. H_2O_2 Electrochemical Detection by Enzyme-Based Modified Electrodes

Considering that H_2O_2 is a product of some oxidases' catalytic activity [26], biosensing of H_2O_2 , based on its electrochemical oxidation/reduction, is frequently favoured by the presence of some specific biological molecules with high peroxidase activity [45]. Accordingly, H_2O_2 biosensing is commonly performed using a protein/enzyme-based modified electrode, depending on the biomolecule supported. Monitoring H_2O_2 by its redox reaction becomes faster, more sensitive, and selective when performed in certain heme-proteins such as haemoglobin or other natural enzymes such as the horseradish peroxidase and heme-containing enzymes, such as cytochrome-c peroxidase [45].

Moreover, given that H_2O_2 is a bioactive molecule, resulting as a by-product of numerous enzyme-catalysed reactions, it renders H_2O_2 a "reporter" molecule that might be used to identify other biomolecules, thus enabling the electrochemical detection of other non-electroactive metabolites [46]. Consequently, considerable attention has been given to the research and design of new, more sensitive electrodes that address H_2O_2 detection and improve the detection of non-electroactive species labelled by H_2O_2 quantification. In this scope, the detection of H_2O_2 by enzyme-based biosensors is of great importance, as H_2O_2 provides the indirect detection of many non-electroactive targets otherwise implausible to be measured. The glutamate and adenosine neurotransmitters are some inactive targets [47,48]. Specific oxidases are immobilised onto the electrode surface, converting the non-electroactive biological target to H_2O_2 for the subsequent in vitro detection of the attendant targeted molecule. This type of screening has been mainly used in the enzymatic detection of glucose by involving glucose oxidase (GOx) assistance in biosensing due to their crucial role in controlling glucose in diabetic patients [49].

However, certain constraints are related to the use of biological material for the analytical detection of H_2O_2 . Namely, the not-always easy process of enzyme-immobilisation [50], the requirement of some molecules on modified electrodes, a mediator between target species and the electrode surface, and the choice of material used as a matrix to restrain molecules on the electrode [51].

Although enzyme-based detection is still a dominant bioanalytical process, this procedure has several shortcomings, such as its complexity, lack of stability, and high cost [52]. This hindrance happens because the enzymatic activity is affected by temperature, pH, atmospheric O_2 and the enzyme's intrinsic nature, leading to enzymatic degeneration, resulting in poor stability and low reproducibility of enzymatic biosensors. Considering all the previously reported issues, developing enzyme-free H_2O_2 sensors has become highly desirable.

2.3. H_2O_2 Electrochemical Detection by Metallic Nanoparticles-Based Electrodes

The development of different modified electrodes for the detection of H_2O_2 has attracted a great deal of attention since the selectivity of the electrochemical response to H_2O_2 occurrence is improved by using various components catalytically active in this modification. Numerous modified electrodes without any enzymes or other proteins

immobilisation have already been reported for the electrochemical detection of H_2O_2 [53]. In particular, metallic-based electrodes have shown excellent catalytic activity towards both H_2O_2 redox reactions [54]. Under this scope, over recent years, research has been performed [55] to evaluate the most suitable materials to apply on the electrode surface to attain the most proficient electrochemical detection of H_2O_2 .

Current research regarding the electrochemical detection of H_2O_2 focuses on the survey for the most efficient electrocatalytic materials, aiming for H_2O_2 direct sensing.

Recent development in nanoscience has brought the proliferation of nanomaterials with essential roles in several areas such as catalysis, sensors, biomedicine, biological labelling, surface-enhanced Raman scattering, and microelectronics [56]. This remarkable growth in nanomaterial research was mainly due to these materials' unique chemical, physical, and electronic properties at their nanoscale. In practice, the difference in the solid materials' properties according to their scale stems from the valence band and conduction band's energy levels gap, which are involved in the chemical bonding of the several atoms composing their structure. As the material's size grows nearer to the electron transfer free path, electrons' transfer between the atoms that constitute that material becomes more unlikely as the d-bands are further apart. Thus, unlike bulk material, the nanomaterial features discrete energy levels due to the constraint of the electrons' wave-function caused by their limited physical dimensions. Accordingly, these unique characteristics are reflected in the exceptional electrical, thermal, catalytic, and optical properties that differ from those of the same bulk materials. On the other hand, nano-sized structures efficiently expose their high specific electrochemical active surface area (ECSA) to connect with the substrate molecules.

The metallic nanoparticles exhibit exceptional capabilities in the catalysis field, mainly due to their high surface-volume ratio and high crystallinity level, which provides the necessary conditions for higher catalytic performance. This property is responsible for the increased number of active sites for electron transfer, making the catalytic approach more efficient. Therefore, metallic nanoparticles are widely used for direct electron transfer in sensor and biosensor devices [57]. The adoption of new surface analysis approaches and the feasibility of structural relationships' modelling of desired materials has enabled the construction of advanced electrodes with tailor-made metal nanoparticles [58].

A reliable catalyst consists of a material that reduces the overpotential required for the electrochemical reaction and improves the kinetics of its electron transfer. In this context, carbon-based materials have revealed high catalytic activity for oxidation and reduction of H_2O_2 . Some of the most frequently used carbonaceous [59] are graphite, glassy carbon, reduced graphene oxide, carbon nanotubes, and carbon paste electrodes.

Simultaneously, metallic nanoparticles on modified electrodes increase the electrocatalytic activity for H_2O_2 detection since they significantly improve the electrode signal [60]. One of the common characteristics of metals is their susceptibility to donate and accept electrons from their valence orbital, readily submitting to the redox process. Specifically, transition metals tend to acquire multiple valence states so that they undergo dynamic transitions between these valence states. This remarkable ability renders transition metals a type of material able to operate as an electron-carrier species during oxidation–reduction reactions.

The transition metal nanoparticles' properties induce rapid mass transport and electron transfer during the heterogeneous electrocatalytic process, causing catalysis at the electrode surface to be very effective. Therefore, the signal amplitude of a nano-metallic composite electrode might result from a concerted action between the atomic structure of the metals and the nano-sized material's specific properties. Due to its relative-inert nature, noble metal nanoparticles are preferred over other transition metal compounds to construct catalytic materials. Considering d-subshell electrons' higher exposure, the dissociative adsorption of adsorbent species on its surface becomes more expedited.

Among the most recently studied metallic nanoparticles, platinum nanoparticles (Pt NPs), single or mixed with other species, disclose a high catalytic effect on the oxygen reduction reaction. Specifically, in heterogeneous catalysis, platinum nanomaterials have

been comprehensively analysed as promising materials since their' porosity additional feature enhances their electrochemical active surface area and consequently sustains the electron transport capacity [61].

Over the last 30 years, platinum nanoparticles (Pt NPs) have been extensively studied in electrochemical applications [62], given their high electrocatalytic efficiency and selectivity. Since mid-2015, Pt NPs-based electrodes have been widely used in the enzyme-free sensing of H_2O_2 [63] due to their high electrocatalytic activity and selectivity for H_2O_2 . Most Pt NPs-based non-enzymatic sensors exhibit an excellent response to H_2O_2 with a wide linear range, low detection limit, and good stability. In addition, the detection of H_2O_2 at low potential will lead to good selectivity.

Although noble metals exhibit good catalytic performance, their high cost and poison susceptibility [64] limit their potential for large-scale applications and emphasise the demand for alternative, less expensive and readily available high-efficiency catalytic materials. One of the biggest threats to platinum catalytic performance is CO contamination during heterogeneous catalysis. This interference results from the molecular structure of CO, whose triple bond justifies the strong binding capacity on the platinum surface, hindering the analyte from accessing the active catalytic sites available for heterogeneous catalysis [64]. However, the platinum electrocatalyst's tolerance to carbon monoxide poisoning can be improved by doping the platinum with other materials such as transition metals [65], oxides or high-surface-area carbonaceous such as multi-walled carbon nanotubes [66]. The incorporation of a different transition metal in the platinum surface structure contributes to the attenuation of CO poisoning due to the alteration of the local electronic structure of platinum at the reaction active site. The resulting hybridisation between the d orbitals of the transition atoms in the alloy reduces the energy of platinum d- orbitals contributing to the rise in CO binding energy, weakening it. Moreover, under the inclusion of a highly oxophilic transition metal (high binding affinity for oxygen), the additional bifunctional effect contributes to CO poisoning surpass. Since at a lower potential, it can oxidise water molecules into hydroxyl species (OH), which react with the CO adsorbed on the adjacent Pt sites, forming CO_2 and H_2 that are released, regenerating the active sites of Pt [67]. On the other hand, CO poison adsorption at the Pt surface was also observed by the modification of Pt electrodes with metallic oxides or carbonaceous that, while increasing the dispersion of PtNPs in the composite structure, breaking the required contiguity of Pt active sites for the adsorption of CO [66].

Since the early first decade of the 21st century [41], many Pt-based bimetallic alloy nanoparticles have been suggested to construct H_2O_2 electrochemical sensors.

In general, Pt NPs exhibit good electrocatalytic behaviour towards the H_2O_2 electrochemical reduction. Likewise, they have been widely used at negative potentials, i.e., under cathodic polarisation conditions, preventing possible interferences of the coexisting electroactive species, such as ascorbic acid (AA) and uric acid (UA) [68]. Nevertheless, despite the catalytic activity toward H_2O_2 reduction reaction, some Pt NPs-modified electrodes might face an interference of dissolved O_2 under cathodic conditions, which is difficult to overcome due to its highly negative reduction potential [69,70].

The introduction of an extra atom to the solid platinum structure usually shifts the electrical potential to more negative values, which most often aids in avoiding the possible interferences from concomitant species in the analyte solution [70,71].

Whenever possible, adjustments to the electrode are desirable by incorporating several materials to increase the catalytic effects resulting from such materials' synergy. Some materials have shown distinct advantages over conventional materials for H_2O_2 detection when combined, adapted, or rearranged. Several H_2O_2 sensing' electrodes are illustrated in the graphical diagram from Figure 1.

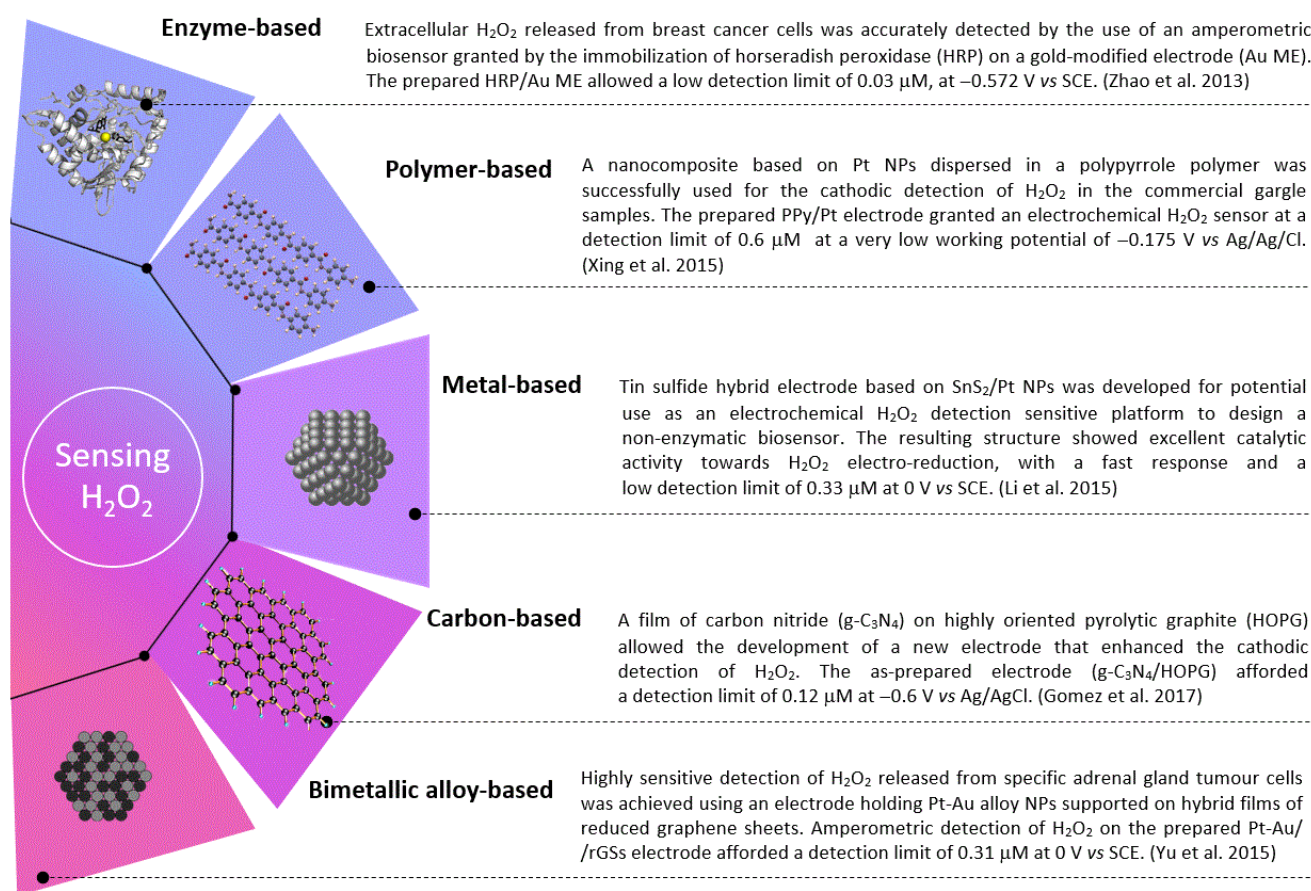


Figure 1. The different electrodes commonly used for the sensitive detection of H_2O_2 . Collected data from the research works of Zhao et al. [35], Xing et al. [86], Li et al. [63], Gomez et al. [59], and Yu et al. [69].

By setting a recognition element of a new sensor, the new electrode is designed by assembling a structure composed of several different compounds, nanoparticles, oxides, and metals collected to outline a new platform on the surface of the electrode. The new electrode platform is accomplished by supporting the electrocatalyst on the electrode surface.

2.3.1. Pt-Based Nanocomposite Structures

Pt-based nanocomposite systems with NPs of different structures (alloyed NPs, mixed monometallic NPs, or core-shell NPs) have proved to be novel architectures with remarkably improved catalytic activity. Therefore, they are used extensively as electrodes for methanol oxidation and oxygen reduction reactions in fuel cell technology [72]. Moreover, bimetallic alloys in sensor development have also been progressing by taking advantage of synergistic effects resulting from metals used in the alloy [73].

For instance, Niu et al. [74] proposed the formation of some nanoclusters with excellent catalytic performance for the reduction of H_2O_2 by the deposition of Pt-Pd nanoagglomerates on gold nanofilm substrate (SPGFE/Pt-PdBNC). The prepared 3D electrode showed a higher current response concerning the H_2O_2 electrochemical reduction in a neutral environment than the monometallic Pt and Pd nanomaterials. After successive addition of H_2O_2 in 0.1 M PBS ($\text{pH } 7.0$), the amperometric results showed that the current values increase linearly with H_2O_2 concentrations ranging from 0.005 to 6 mM . The snowflake-shaped Pt-Pd alloy nanostructure carries more catalytic sites for H_2O_2 reduction, thus making it more sensitive to the addition of low concentrations of H_2O_2 at $0.4 \text{ V vs. Ag/AgCl}$ at the $804 \mu\text{A mM}^{-1} \text{ cm}^{-2}$ measurement.

Mei et al. [75] have prepared a novel sensor based on Fe@Pt/C core-shell core-shell nanocomposites with excellent catalytic activity toward H₂O₂ reduction. The Fe@Pt core-shell structures with a thin Pt shell layer on the non-noble metal core were synthesised by a sequential reduction process and subsequent Fe@Pt/C by the dispersion of bimetallic NPs on Vulcan XC-72 carbon. The voltammetric results suggest that the Fe@Pt/C provided the necessary conduction pathways to promote the electron transfer rate and the Fe@Pt NPs-modified electrode has a wide ECSA. The new sensor based on Fe@Pt/C nanocomposites exhibited an excellent catalytic activity for reducing H₂O₂ at a working potential of -0.4 V vs. saturated calomel electrode (SCE), emphasising its practical utility for H₂O₂ sensing. The results have shown that the Fe@Pt/C electrode displays good catalytic activity for H₂O₂ with high sensitivity, good stability and excellent reproducibility. Chronoamperometric measurements showed that the Fe@Pt/C-modified electrode exhibits a sensitivity of $218.97 \mu\text{A mM}^{-1} \text{cm}^{-2}$ and a detection limit of 750 nM from the linear relationship between the reduction current-signal and the concentration of H₂O₂ in the range of $25 \mu\text{M}$ to 41.605 mM. The applicability of the developed sensor was evaluated by verifying the amount of H₂O₂ in an antibacterial lotion (3% H₂O₂). The results are in line with the expected value; thus, the excellent catalytic performance of Fe@Pt/C makes it a promising application for H₂O₂ quantification. The improved catalytic performance of Fe@Pt [75] results from the electronic and structural effects [76] between a metal core and the shell of bimetallic core-shell NPs. This phenomenon can be ascribed to electronic effects since the electronegativity of Fe is lower than that of Pt, thus altering the electronic properties of Pt when the metals are adjacent as Fe@Pt-skin. Thus, nearby Fe, the density of the Pt d-band is reduced to lower energy [77], leading to a change in the chemical adsorption energies. Moreover, the induced modification of the electronic structure of Pt-skin by Fe can increase the number of active sites for analyte adsorption [77].

In addition, the group Zhao et al. [68] have prepared a high porous composite of core-shell Cu@Pt/C nanoparticles structure. Such an open-cell organisation with irregular pores has allowed them to provide a higher number of active sites to adsorb the analyte H₂O₂ and thus improve their electrocatalytic activity. The analysis performed by CV and XRD techniques shows that the improved electrocatalytic performance associated with Cu@Pt NPs is due to the structural and electronic modification of the Pt atoms near the surface/shell layer caused by the Cu core. X-ray diffraction (XRD) analysis shows that the Pt at the bimetallic core-shell particle surface exhibits lower binding energy in Cu@Pt NPs than the bulk Pt. The electrochemical survey showed that the currents obtained for H₂O₂ reduction increase gradually with increasing H₂O₂ concentration, indicating that Cu@Pt/C/GCE can be used to quantify H₂O₂ concentration. Compared to Pt/C, Cu@Pt/C has revealed better electrocatalytic activity for H₂O₂ reduction, showing a sensitivity of $351.3 \mu\text{A mM}^{-1} \text{cm}^{-2}$ and a limit of detection of $0.15 \mu\text{M}$ over a wide linear range of H₂O₂.

2.3.2. Pt-Based@ Carbonaceous Structures

Carbonaceous is one of the most suitable materials to support the catalysts for a high-sensitivity sensor due to its characteristics, such as large surface area, porous structure, and good electrical conductivity [78]. Carbon-based materials are essential as they influence the kinetics and mechanism of the redox reaction at the electrodes. Generally, the kinetics of the electron transfer process in carbon-supported electrodes relies on the carbon structure and its surface treatment. However, the highly hydrophobic nature of carbonaceous makes them suitable for a superior catalytic activity in biosensing applications. Carbonaceous are low-cost support materials whose availability and simple removal from the electrode surface make them a favourable support platform for electrochemical measurements. Additionally, carbon-based electrodes have a high chemical and electrochemical stability over an extensive potential range in the negative and positive directions.

Zhao et al. [79] have developed a modified electrode by the electrodeposition of Pt NPs in flowers shape on Fe oxide supported on reduced graphene oxide (Fe₃O₄/rGO). Such electrocatalyst has proven to be a reliable and effective tool for H₂O₂ detection. The

experimental CV shows that the current intensity on Pt/Fe₃O₄/rGO/GCE increased with H₂O₂ in 0.1 M PBS (pH 7.4), highlighting the rapid electron transfer at the electrode interface during the H₂O₂ reduction. From the impedance assays was also possible to check that the electrical resistance decreased as the various electrode sub-layers increased, from GCE > Fe₃O₄/GCE > Fe₃O₄/rGO/GCE > PtFe₃O₄/rGO/GCE. It suggests that graphene and Pt nanoparticles may be at the origin of the effective promotion of electron transfer. The amperometric characterisation of Pt/Fe₃O₄/rGO showed a sensitivity of 6.875 $\mu\text{A mM}^{-1}$ from the linear range between 0.1 and 2.4 mM concentration of H₂O₂ and a detection limit of 1.58 μM . Furthermore, the Pt/Fe₃O₄/rGO sensor's behaviour showed a favourable anti-interference characteristic on the coexisting species in biological samples. The electrochemical analysis results suggested that the proposed Pt/Fe₃O₄/rGO electrode could be an effective tool for the quantitative electro-cathodic surveillance of H₂O₂.

Several electrocatalysts with distinct degrees of N-graphene (N-Gr) loading were assembled and used as advanced electrodes for H₂O₂ detection by Tajabadi et al. [80]. The electrode was prepared by electrophoresis of N-graphene nano-sheets on indium tin oxide glass (ITO) substrate, on which nanoflower shaped (NF) Pt nanoparticles were electrochemically deposited. The PtNF-N-Gr has shown a fast amperometric response over a wide linear range of H₂O₂ (1 μM to 1 mM), denoting a high catalytic behaviour of the modified electrode towards H₂O₂ reduction at the working potential of $-0.40\text{ V vs. Ag/AgCl}$. The amperometric response of the 0.05 mg ml⁻¹ of N-graphene loading modified ITO electrode in nitrogen-saturated 0.1 M PBS solution to successive additions of H₂O₂ was used to explore the performance of the as-prepared electrochemical sensor. The hybrid electrode exhibited fast, stable, and reproducible current responses and a linear current response to successive additions of H₂O₂ in the PBS solution. This modified electrode showed the best catalytic performance with a detection limit of 0.34 μM . Electrochemical impedance spectroscopy analysis (EIS) also corroborated the higher catalytic ability of the electrode employing the charge of 0.05 mg ml⁻¹ in N-graphene. This conductivity increment improves the electrocatalyst catalytic capacity, which results in a faster electron transfer process across the interface and better catalytic performance of the electrode when used as a sensor.

2.3.3. Pt-Based@ Highly Porous Structures

The specific surface area of porous architectures relies on the size of their ligaments, their pores, and solid bulk densities [81]. Effectively, the porous material of the electrode has a high ECSA, also known as specific surface area. Moreover, the specific surface area of the porous architecture rises with the number of porous cages. The same goes for rough surfaces. The electrode roughness is the ratio between the electroactive surface area of the electrode and its geometric area. Usually, the roughness factor of nano-sized catalytic material is high as the electrode's specific surface area is much higher than the geometric one. Porous and highly rough electrocatalysts promote heterogeneous electron transfer at the analyte/electrode interface. They provide a wider surface area to react with the analyte and increase the heterogeneous electron transfer. The unique catalytic activity of the platinum surface coupled with the high surface area granted by its roughness provides additional sites for the electrocatalytic reduction of hydrogen peroxide, thereby increasing the reaction rate on the electrode surface.

Effectively, Guo et al. [82] have prepared an electrode based on the coaxial nano-cables, which can readily adsorb high-density metal nanomaterials through the functionalisation with an NH₂ group. Thus, this group formulated an electrode modified with a high roughness CNT/SiO₂/(Au/Pt) nanostructure that showed improved catalytic skills towards the direct reduction of H₂O₂ at $-0.15\text{ V vs. Ag/AgCl}$, reaching the maximum cathodic constant current within 3.5 s. This swift performance was ascribed to the fact that H₂O₂ is readily diffused within the high ECSA of the CNT/SiO₂/(Au/Pt) where it will react. The CV study verified that H₂O₂ cathodic peak currents increased with both concentration of H₂O₂ in 0.1 M PBS (pH 7.0) and scan rate from 0.02 to 0.2 V s⁻¹. The amperometric analysis

also disclosed a sensitive linear response of the modified electrode towards the H_2O_2 electroreduction from 0.5 μM to 1.67 mM, with a detection limit of ca. 0.3 μM . Moreover, such ultra-high-density Au/Pt NPs modified electrodes showed a high performance in the electro-oxidation of oxygen, methanol, and hydrazine.

A sensitive and selective amperometric detection of H_2O_2 in biological samples was accomplished by a new electrode prepared by Thirumalraj et al. [83] through the electrochemical deposition of Pt NPs on a mixture of graphite (Gr) and gelatin (GLN) protein. The combination of the high catalytic performance of graphite with the excellent matrix of the protein molecules comprising the gelatin makes the resulting hydrogel into a perfect immobilising platform for various biomolecules detection. The modified electrode PtNPs@GR/GLN showed an excellent electrochemical behaviour over H_2O_2 sensing with high electrocatalytic activity at a lower working potential for H_2O_2 reduction. Therefore it allowed the development of a non-enzymatic sensor for the selective detection of H_2O_2 in the presence of other biologically active interfering molecules such as AA, DA, and UA at a low detection limit of 37 nM. The superior dispersing action of GNL on high catalytic GR layers increases the number of active sites available in the electrode matrix. As a result, it fosters a heterogeneous electron transfer process at the interfaces of electrode/electrolyte. PtNPs@GR/GLN was successfully applied to electrochemical monitoring of H_2O_2 in biological samples of human serum and saliva.

2.3.4. Pt-Based@ Conductive Polymer Structures

Conductive polymers are π - π -conjugated polymers [84] containing functional groups that allow the easy immobilisation of the recognition molecules. In general, conductive polymers have unique features, such as high electrical conductivity resulting from the delocalised π -electrons within the polymeric chain backbone and low ionisation potential. Commonly, metallic nanoparticles or metal oxides can be immobilised on the polymer structure, resulting in stable hybrid films of high catalytic activity. These large surface areas, high conductivity, and reduced charge/mass transport pathways sustain the potential success of conductive polymers as catalyst supports for electrochemical sensing devices.

Within the energy field investigation, Oliveira et al. [85] have prepared several polypyrrole/platinum composites tested for the cathodic reaction of H_2O_2 in acidic media. Pt-based assembled electrocatalysts supported conductive polypyrrole-carbon composite (PPy-C) containing different amounts of carbon black (5, 12, 20, 35%). Among the four electrocatalysts, Pt/PPy-C_{35%} exhibited the best electrochemical response toward the H_2O_2 cathodic reaction, showing a remarkable current density peak of 11.6 mA upon the addition of H_2O_2 to the supporting electrolyte at a relatively low potential of 0.8 V vs. RHE. The improved catalytic performance of Pt/PPy-C_{35%} for H_2O_2 cathodic reaction was sustained by the lower activation energy value than the remaining catalysts.

In the scope of non-enzymatic H_2O_2 detection, catalysts prepared and evaluated by various researchers have also been assessed as new sensors for H_2O_2 in different commercial samples [75] and at a cellular level [83].

For example, Xing et al. [86] have developed an electrochemical H_2O_2 sensor made of a polypyrrole/platinum composite, with platinum nanoparticles densely dispersed within those of PPy. This PPy/Pt electrocatalyst evidenced good catalytic activity towards H_2O_2 reduction, with an enhanced detection sensitivity at a lower working potential (c.a. -0.175 V vs. Ag/AgCl). Indeed, at this low working potential of -0.175 V, no significant current response was observed owing to the reduction of the coexisting O_2 , not affecting the electrochemical detection of H_2O_2 . The sensor calibration curve shows a sensitivity of $305.45 \mu\text{A mM}^{-1} \text{cm}^{-2}$ over the linear range of 25 to 500 μM H_2O_2 and a detection limit of 0.6 μM . The PPy/Pt/GCE sensor used to construct a non-enzymatic electrochemical H_2O_2 detector showed superior sensitivity, selectivity, and accuracy. It was also successfully applied to detect H_2O_2 in commercial gargle samples, proving its feasibility in practical analysis.

2.3.5. Pt-Based Bimetallic Alloys

The second atom within the electrocatalyst provides a vital strategic variation in its shape, size, and morphology, resulting in the amendment of its chemical and physical properties. Effectively, adding a second element to the metallic structure provides the synergistic effect of both materials, along with a cost reduction in the electrocatalyst due to the decline in the amount of most expensive metal, e.g., platinum [64]. Compared with the corresponding mono-metal NPs, bimetallic blends reveal higher catalytic activity, more reliable resistance to deactivation, and excellent catalytic selectivity.

Over the past two decades, several research groups have successfully developed different catalytic materials [41,73] based on Pt and transition-metal alloys targeting the selective detection of H_2O_2 . Table 1 summarises the main analytical parameters of H_2O_2 detection by different Pt-based electrocatalysts developed by several researchers.

Mei et al. [87] have reported the development of a high selective enzyme-free H_2O_2 sensor based on PtNi bimetallic alloy onto multi-walled carbon nanotubes (MWCNTs). It exhibited excellent sensitivity, stability, and reproducibility, making it suitable for detecting H_2O_2 in real samples. The well-dispersed MWCNT granted a higher ECSA for PtNi active species, resulting in a highly electroactive hybrid composite. The improved electrochemical activity of PtNi/MWCNTs is ascribed to the mentioned higher ECSA. Voltammetric measurements performed in Mei's work on the modified PtNi/MWCNT electrode pointed to a diffusion-controlled mechanism for the H_2O_2 reduction reaction on its surface. In practice, PtNi/MWCNTs electrode has revealed higher electrocatalytic activity towards H_2O_2 reduction, along with a unique sensitivity and selectivity for sensing H_2O_2 at the -0.45 V vs. SCE as working potential and pH 7.0. Accordingly, the prepared electrode accomplished a sensitivity of $2123.1 \mu\text{A mM}^{-1} \text{cm}^{-2}$ with a detection limit of $0.06 \mu\text{M}$.

Similarly, Gutierrez et al. [88] have prepared a copper-rich core-shell structure decorated by a PtPd alloy shell supported on a glassy carbon electrode, which revealed substantial electrocatalytic activity for H_2O_2 reduction. The comparison of the modified electrode sensitivities by every single metal separately and by the PtPd alloy around the Cu nanostructure (Cu@PtPd/C) highlights the synergy of the different metals in the final composite for the reduction of H_2O_2 at -0.1 V vs. Ag/AgCl. It also shows a high sensitivity of $530.0 \mu\text{A mM}^{-1} \text{cm}^{-2}$ and a detection limit of $0.37 \mu\text{M}$. The electrocatalyst was used to assemble a sensing platform that was successfully exploited to quantify H_2O_2 in a commercial mouthwash sample. The Cu@PtPd/C structure also shows excellent amperometric durability and long-term stability with good anti-interference for AA and UA in amperometric detection of H_2O_2 at -0.1 V. Furthermore, the voltammetric profiles obtained for 0.050 M H_2O_2 on GCPE paste and 5% *w/w* Cu@PtPd/C GCPE portray that core-shell NPs decrease both the oxidation and reduction potentials for H_2O_2 . In addition, the significant improvement of the associated currents for both processes highlights the electrocatalytic effect of Cu@PtPd/C for H_2O_2 electrochemical redox reactions.

Under an energy supply-based approach, Morais et al. [18] have prepared the bimetallic electrodes of PtNi and PtCo NPs by immobilising them on a glassy carbon electrode (GCE) surface with a Nafion solution binder. The resulting $\text{Pt}_{0.75}\text{M}_{0.25}$ /Vulcan XC-72 carbon black electrodes showed significant catalytic performance in the electrochemical reduction of 0.03 M H_2O_2 , exhibiting current signals in the milliamperic range. Similarly, the prepared Pt/C, $\text{Pt}_{0.75}\text{Ni}_{0.25}$ /C and $\text{Pt}_{0.75}\text{Co}_{0.25}$ /C electrocatalysts exhibited a rate constant for the cathodic reaction of H_2O_2 of 7.4×10^3 , 11.2×10^3 and $11.8 \times 10^3 \text{ mol}^{-1} \text{cm}^3 \text{s}^{-1}$, respectively, showing a high catalytic performance for H_2O_2 reduction. Therefore, the tested catalysts should also exhibit high electrocatalytic performance and offer an excellent application as sensitive sensors for the physiological estimation of H_2O_2 . In this study [18], the kinetic results showed a superior catalytic activity of carbon-supported Pt alloys for the H_2O_2 electrochemical reduction reaction compared to monometallic Pt. Accordingly, the dependence of catalytic activity on the nature of the alloying component has been shown so that, for instance, catalytic activity increased in the following order: $\text{Pt}_{0.75}\text{Co}_{0.25}/\text{C} > \text{Pt}_{0.75}\text{Ni}_{0.25}/\text{C} > \text{Pt}/\text{C}$.

Similarly, Cardoso et al. [89] have investigated different rare earth and platinum alloys (Sm, Dy, Ho) in an alkaline medium. The cyclic voltammetry analysis (CV) for 0.05 M H_2O_2 in 2 M NaOH solution at -0.1 V vs. reference hydrogen electrode (RHE) showed a higher current signal for the Pt-Sm alloy. There is strong evidence that these current density values attained may be related to the significant roughness of the Pt-Sm alloy surface and the increased active sites for the catalytic reaction.

By 2018, Guan et al. [90] prepared a PtNi(3:1) alloy on N-doped carbon nano-fibres by electrospinning that exhibited an excellent sensitivity of $248.5 \mu\text{A mM}^{-1} \text{cm}^{-2}$ towards the reduction of H_2O_2 in an electrolyte of pH 7.24 standardised by PBS, reaching a relatively low limit of detection of $0.0375 \mu\text{M}$. The studied nanocomposite alloy presented a high catalytic performance at a relatively low potential of -0.5 V vs. SCE, with the reduction current reaching $-350 \mu\text{A}$. The decay of the transient current, observed under a chronoamperometric analysis of the 1.0 mM H_2O_2 reduction reaction on PtNi/NCNFs/GCE, pointed to a diffusion-controlled process. This process allowed Cottrell's expression to apply to obtain the catalytic rate constant for H_2O_2 reduction as $3.13 \times 10^4 \text{ mol}^{-1} \text{ s}^{-1}$. The resulting prepared electrode exhibited a progressive reduction current response with increasing the concentration of H_2O_2 (Figure 2a) in a rapid, sensitive (Figure 2b) and selective (Figure 2c) way.

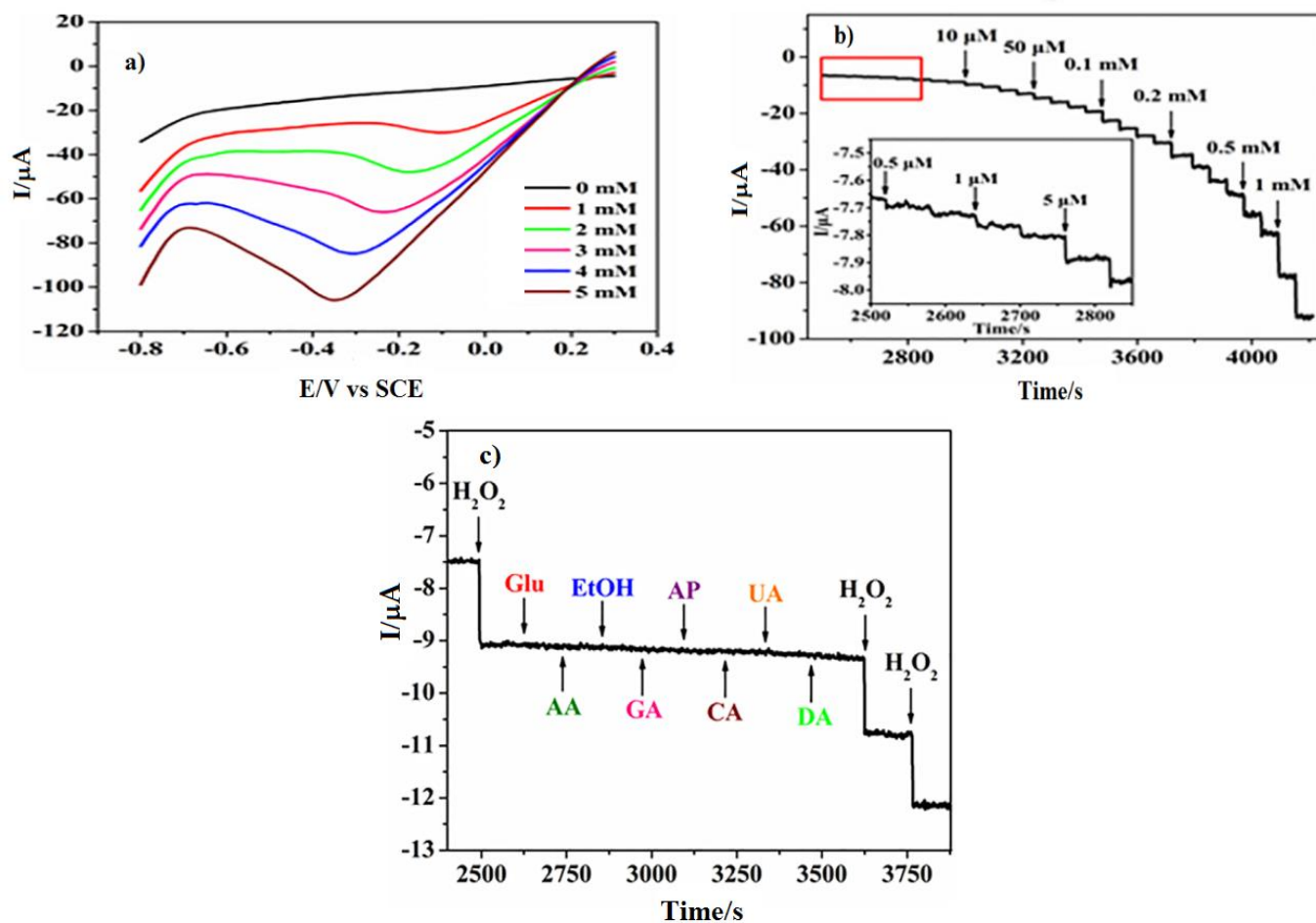


Figure 2. (a) Linear Sweep Voltammetry of the PtNi/NCNFs (3:1)-GCE electrode at different H_2O_2 concentrations. (a) Current-time response of PtNi/NCNFs (3:1)-GCE to the successive additions of H_2O_2 at -0.1 V. (b) Amperometric response curve at PtNi/NCNFs (3:1)-GCE to successive additions of 0.1 mM H_2O_2 and other electroactive species at -0.1 V (c) in 0.2 M N_2 -saturated PBS. Adapted from Guan et al. [90], Copyright 2018 Elsevier.

As one of the most promising metal oxides in respect of its electrocatalytic performance toward H_2O_2 reduction, rare-earth oxides CeO_2 grants a high electrical conductivity and the ability to mimic the activity of several natural redox enzymes. Although, the aggregation of CeO_2 -based nanocomposites declines their catalytic activity, limiting their efficient use. Considering this, Guan and coworkers [91] have developed a relevant procedure that enables the incorporation of CeO_2 into nanocomposites through their anchoring on the surface of N-doped carbon nanofibers. Therefore, they have prepared a catalytic material that uniformly embeds the PtNi alloy/ CeO_2 plates onto high surface N-doped carbon nanofibers (PtNi/ CeO_2 /NCNFs) with an exceptional sensitivity of $345.0 \mu\text{A mM}^{-1} \text{cm}^{-2}$ towards the cathodic reaction of H_2O_2 . CV studies revealed that PtNi/ CeO_2 /NCNFs electrode yielded a much higher reduction current density of $-506.5 \mu\text{A}$ at a potential 0.1 V lower than the previously-synthesised PtNi/NCNFs/GCE [90]. The diffusion-controlled mechanism of the H_2O_2 reduction reaction was observed at the prepared PtNi/ CeO_2 /NCNFs/GCE surface. The catalytic rate constant of the cathodic reaction of 1.0 mM H_2O_2 on the prepared electrode was as high as $3.52 \times 10^4 \text{ mol}^{-1} \text{ s}^{-1}$.

In the H_2O_2 electrochemical oxidation domain, Yang et al. [92] have prepared a porous structure of nanoparticles' PtCu alloy that has an interconnected flower-like network skeleton that exhibits an outstanding detection performance towards H_2O_2 and glucose (GLU) electrochemical oxidation in near-neutral pH solutions. Particularly for H_2O_2 electrochemical oxidation, the prepared nanoporous material required a low working potential of 0.7 V vs. RHE and granted the detection of H_2O_2 in trace amounts as low as the detection limit of 0.1 μM . Over the range between 0.5 and 1.2 V, the PtCu alloy electrode onset potential is negatively shifted by more than 170 mV. It also reveals a superior catalytic activity for the electro-oxidation of H_2O_2 than Pt/C. The voltammetric behaviour of the PtCu alloy electrode towards the anodic reaction of the glucose has displayed a current density about 20 times higher than the obtained for the commercial Pt/C electrode.

Within the context of detecting endogenous H_2O_2 , hybrid films based on bimetallic nanoparticles supported on reduced graphene sheets were prepared by Yu et al. [69] at various molar ratios of each metal. The sensor assembled by the prepared electrocatalyst has shown to be highly selective and sensitive to H_2O_2 electroreduction. Bimetallic Pt-Au/rGSs hybrid films have afforded the amperometric detection of H_2O_2 at a low potential of 0.0 V vs. SCE, with a detection limit of about 0.31 μM . All the anodic interferences resulting from electroactive species such as AA, UA, and dopamine (DA), as well as the cathodic interference from endogenous O_2 , were avoided at this low working potential. This type of metallic blend provides a comprehensive linear response to H_2O_2 and excellent selectivity. Therefore, the prepared sensor was successfully used to detect H_2O_2 released from PC12 pheochromocytoma cells and thus showed to be a promising alternative for in vivo H_2O_2 monitoring in the diagnostics domain [69].

In 2017, Hong Li et al. [93] developed a carbon fibre microelectrode (CFME) with a sensitive Pt-Pd alloy for H_2O_2 detection by electrochemical deposition. The microelectrode, whose nanocoral-shaped alloy possesses a high active surface favourable for a fast and efficient electron transfer, grants it a superior catalytic activity for H_2O_2 detection. Under ideal conditions, the prepared Pt-Pd/CFME microelectrode showed excellent response time (≤ 5 s), a high sensitivity ($11,600 \mu\text{A mM}^{-1} \text{cm}^{-2}$), and a low detection limit (0.42 μM) under a wide linear range (5–3920 μM) for H_2O_2 detection. Furthermore, the prepared microelectrode was successfully used in a sensor to monitor H_2O_2 at the cellular level, namely from A549 epithelial cells and the amount of H_2O_2 in milk.

Table 1. Summary of main literature analytical parameters of various Pt-based alloy/bimetallic catalysts towards the electrochemical reduction of H₂O₂.

Electrocatalyst	Cyclic Voltammetry			Amperometry			Ref.	
	E _{pc} (V)	I _{pc} (μA)	E _{working} (V)	K _{cat} (mol ⁻¹ cm ³ s ⁻¹)	Linear Range (mM)	Sensitivity (μA mM ⁻¹ cm ⁻²)		Detection Limit (μM)
SPGFE/Pt-PdBNC	-0.05/Ag/AgCl	400.0 (10.0 mM H ₂ O ₂)	-0.40		0.0050–6.00	804.0	0.870	[74]
Fe@Pt/C	-0.55/Ag/AgCl	300.0 (20.0 mM H ₂ O ₂)	-0.40		0.0025–0.0416	218.9	0.750	[75]
Pt _{0.75} Ni _{0.25} /C	0.53/Ag/AgCl	1075.2 (30.0 mM H ₂ O ₂)	-0.20	11.2 × 10 ³ (30.0 mM H ₂ O ₂)				[18]
Pt _{0.75} Co _{0.25} /C	0.37/Ag/AgCl	1274.0 (30.0 mM H ₂ O ₂)	-0.20	11.8 × 10 ³ (30.0 mM H ₂ O ₂)				
Pt-Sm	-0.40/RHE	2025.0 (50.0 mM H ₂ O ₂)	-0.40					[89]
Pt/Fe ₃ O ₄ /rGO	0.00/SCE	20.0 (0.2 mM H ₂ O ₂)	0.00		0.1000–2.40	0.973	1.580	[79]
PtNi/NCNFs(3:1)	-0.50/SCE	350.6 (20.0 mM H ₂ O ₂)	-0.10	31.3 × 10 ³ (1.0 mM H ₂ O ₂)	0.0005–8.00	248.5	0.0375	[90]
PtNi/CeO ₂ /NCNFs	-0.40/SCE	506.5 (20.0 mM H ₂ O ₂)	-0.10	35.2 × 10 ³ (1.0 mM H ₂ O ₂)	0.0005–15.00	345.0	0.025	[91]
CNT/SiO ₂ /(Au/Pt)	-0.15/Ag/AgCl	23.0 (1.5 mM H ₂ O ₂)	-0.10		0.0005–1.67		0.300	[82]
Pt NF-N-Gr	-0.40/Ag/AgCl		-0.40		0.0010–1.00	61.23	0.340	[80]
Pt/PPy-C35%	0.80/RHE	11,600.0 (50.0 mM H ₂ O ₂)	0.90					[85]
PtNi/MWCNTs	-0.40/SCE	275.0 (10.0 mM H ₂ O ₂)	-0.45		0.0002–24.60	2123.1	0.060	[87]
Cu@Pt/C	-0.30/SCE	310.0 (20.0 mM H ₂ O ₂)	-0.30		0.0005–32.56	351.3	0.150	[68]
np-PtCu	0.30/RHE		0.70		0.0100–1.70	64.7	0.100	[92]
PPy/Pt	-0.175/Ag/AgCl	180.0 (4.0 mM H ₂ O ₂)	-0.175		0.0250–0.50	305.45	0.600	[86]
Cu@PtPd/C	-0.10/Ag/AgCl		-0.10		0.0050–0.25	530.0	0.370	[88]
Pt-Au/rGSs	0.10/SCE	35.0 (0.1 mM H ₂ O ₂)	0.00		0.0010–1.78	0.735	0.310	[69]
Pt-Pd/CFME	-0.50/Ag/AgCl	7.7 (5.0 mM H ₂ O ₂)	-0.40		0.0050–3.92	11,600.0	0.420	[93]
PtNPs@GR/GLN	0.16/Ag/AgCl		0.14		0.00005–0.871	5643.0	0.037	[83]

Where K_{cat} is the rate constant of the cathodic reaction of H₂O₂ in each of the electrocatalysts used.

In addition to the easy release of competing analyte species from the active sites on the platinum surface, the extra atom in the alloy also changes the working potential of the nanocatalysts for H_2O_2 detection. Generally, the added atom in the platinum alloy interacts with platinum atoms, altering the electron energy levels in the alloy in such a way that the downshift in the energy of the substrate d-band centre changes the energy bond from the platinum d orbital. This way, it shifts the working potential towards potential values closer to zero, allowing the sensing of H_2O_2 at potentials where the coexisting species show a negligible electrochemical signal.

The optimised performance of some electrocatalysts allowed the selective detection of H_2O_2 among experimental samples having other concurrent bioactive species commonly present in biological fluid samples. For example, ascorbic acid (AA), uric acid (UA), dopamine (DA), glucose (GLU), and acetaminophen (AAP), which are regularly present in biological fluid samples, and other common metal ions such as NO_2^- , SO_4^{2-} , and Cl^- were added for measure along with the H_2O_2 [68,74,75,79,83,87,88,92,93]. The negligible current value verified for those electroactive species revealed an excellent selectivity of the reported electrodes towards the reduction of H_2O_2 .

3. Electrocatalysts' Intrinsic Catalytic Activity toward H_2O_2 Reduction

In the sector of the electrochemical detection of hydrogen peroxide, the main factor leading to the effective screening of low levels of H_2O_2 is the performance of the sensor's transducer element. It corresponds to the electrode surface where the electrochemical reaction takes place.

Upon the catalytic action of an electrode, the H_2O_2 reduction reaction is likely to exhibit lower activation energy, thus improving its kinetics. Electrochemically, a lower overpotential at a specific current density should also be observed. As the most active precious metal against most chemical reactions in both acidic and alkaline electrolytes, platinum is the best known and most widely used catalyst. As a result of the d-orbital electron structure on the surface of its atoms, platinum induces a temporary binding of other molecules. Upon the adsorption of other molecules, the overall shape of the electronic cloud is rearranged so that the adsorbed molecules reassemble into new compounds. After the rearrangement, those molecules are driven off by other new inputs, but the electron structure of platinum as a catalyst does not change. Platinum's low reactivity and valence band suitable for slow and weakly polar bonds with other atoms (mainly H and C) make its polycrystalline surface a good platform for the catalytic assignment of different reactions. As an excellent catalyst, platinum promotes the electrochemical reaction on its surface at a lower pressure and temperature in a shorter reaction time without being involved in it.

As mentioned above, despite its outstanding catalytic performance, platinum suffers from some significant drawbacks. One concerns the deactivation process of its catalytic activity by the adsorption of CO or some other reaction intermediates molecules to the Pt surface, blocking the active sites for heterogeneous catalysis [94]. Another drawback of bulk platinum as a catalyst material is its high cost. Platinum is scarce among precious metals. According to the market and consumption website Statista [95], the average worldwide platinum extraction represents only 170 metric tons in 2020, compared to other precious metals readily mined in more places such as gold (3030 tons) and silver (23,500 tons). Therefore, platinum trades at higher prices per unit based on its demands. In the prospect of a cost-effective electrode of comparable or superior catalytic performance, the construction of electrocatalysts by the fusion of various catalytic materials has been underway for half a century. The nature of the surface of bimetallic systems has been the subject of considerable research over the last forty years, considering these materials' high catalytic activity and selectivity compared to their single metal counterparts [62].

Scientific findings related to Pt nanocomposite-based sensors for the sensitive detection of H_2O_2 highlight the enhanced catalytic effect achieved owing to the coexistence of other elements in the hybrid Pt composites. The improved catalytic performance of the Pt-based bimetallic alloys for H_2O_2 reduction is justified under two aspects:

1. Catalyst' active surface area;
2. Synergistic effects of catalyst mixture.

3.1. Catalyst' Active Surface Area

A bimetallic catalyst exhibits a larger active area, providing more active sites for breaking the molecular bonds and establish new bonds during catalysis than their single metallic counterparts. In practice, the reallocation of active sites on the surface of the electrocatalyst on account of its larger ECSA concerning its nominal area leads to an increase in catalytic activity.

Along with the extra atom in the platinum alloy, hybrid films with carbon allotropes provide extensive surface areas for uniform and homogeneous well-dispersed deposition of platinum nanoparticles. Moreover, including a generous and highly porous structure of carbon material in the Pt nanocomposite configuration will provide a larger adsorption area for the species that will undergo catalytic conversion. Such is the case for carbon allotropes of ordered mesoporous structure (Gr, rGS, and rGO) [69,79,80,83], organised carbon fibres [90,91,93], or even 1D planar structures of CNTs and MWCNTs [82,87].

In addition to mesoporous carbon structures, the high porosity silica (SiO₂) also assembles a 3D support for the ultra-high density Au nanoparticles [82], expanding the extent of the ECSA for the catalytic reaction to occur, thus providing a sensitive response for the detection of H₂O₂ in neutral media (pH 7).

Considering the work of Morais et al. about Pt alloys electrocatalysts [18], it is possible to verify the effect resulting from the high distribution of active sites on the electrode surface. An increase in H₂O₂ reduction activity was observed in the Pt_{0.75}M_{0.25}/C alloys by experiencing a higher current density in an effective ECSA smaller than platinum itself. Indeed, the bimetallic cobalt alloy provides twice the current density at potential -0.2 V vs. SCE (19.0 mA cm⁻² vs. 8.0 mA cm⁻²), with about half the specific surface area Pt/C (0.91 cm² vs. 1.63 cm²). It leads to the appraisal of more free active sites on the surface of the Pt_{0.75}Co_{0.25}/C alloy for the H₂O₂ reduction reaction.

Accordingly, research on electrodes with highly irregular surfaces, either of high roughness [82,89] or high porosity [68,87], shows an increase in the electroactive surface available for heterogeneous catalysis of H₂O₂. The rough surfaces provide an additional number of active sites for the electrocatalytic reaction of the analyte, thus increasing the rate of the reduction reaction of the hydrogen peroxide.

3.2. Synergistic Effects of Catalyst-Blend Mixture

The interaction between the various metals comprising the alloy can effectively improve the electrocatalytic activity of the alloy. These bimetallic structures [96] are usually in the shape of core/end nanostructure alloys and mixed-metal nanoparticles. At this stage, the underlying mechanism and the factors that affect the catalytic properties of the bimetallic alloys owing to the addition of the second metal atom in the platinum atomic lattice are not entirely understood. However, some ideas have already been suggested to explain the improved catalytic activity attained by bimetallic catalysts [96]. These are based on the factors that provide a better interaction of the reactant and intermediate species to the catalyst' active sites, i.e., on three different chemical effects that dictate the adsorption energies of the analyte species to the catalyst surface. They are divided into three categories; (i) the geometric factor, (ii) the electronic effect, and (iii) the co-catalytic effect:

- (i). Geometric factor: A change in the surface geometry of the catalyst surface as a result of distance from its nearest neighbour atom (*strain or ensemble effects*);
- (ii). Electronic effect: A change in the reactivity of the catalyst as a result of electron transfer or polarisation between the two adjacent metals, which leads to a change in the width of the surface d-band and a shift in the binding energy aimed at constant band filling (*ligand or electronic effect*);
- (iii). Co-catalytic effect: Upon adding a second metal element in the Pt lattice, it can provide a reinforced adsorption site for some intermediate species or reactants, thereby

enhancing their interaction with the catalyst. It is referred to as a *synergistic* effect because the combined action of both metals fosters improved adsorption to the catalyst. This way reinforces the catalytic ability of the bimetallic NPs.

As mentioned above in the nickel and cobalt alloys research [18], the kinetics of the electroreduction of H_2O_2 in polycrystalline Pt alloys are much more efficient in electrolytes free from other simultaneous highly adsorbing species [97]. Indeed, an enhancement of H_2O_2 reduction activity on Pt-alloys, $\text{Pt}_{0.75}\text{M}_{0.25}/\text{C}$, was observed due to the higher availability of the Pt active site on this kind of electrode surface.

The catalytic performance of carbon-supported electrocatalysts for the cathodic reaction of H_2O_2 directly depends on the electrode reaction rate, which relies on the availability of Pt active sites [18]. H_2O_2 will have to “compete” with other co-adsorbed analyte species capturing the active sites on the Pt surface during its cathodic reaction (Figure 3a). This seizure has an inhibitory effect, delaying the catalytic activity for the cathodic response of H_2O_2 . Thus, the presence of a second metal (similar to that portrayed in Figure 3b) will affect the electronic configuration of the outer Pt atoms at the electrode surface, so the bonds of the adsorbed species on the electrode surface are weakened, helping their removal upon their catalysis (*electronic* effect). It turns available the active Pt sites again for the catalysis of H_2O_2 reduction.

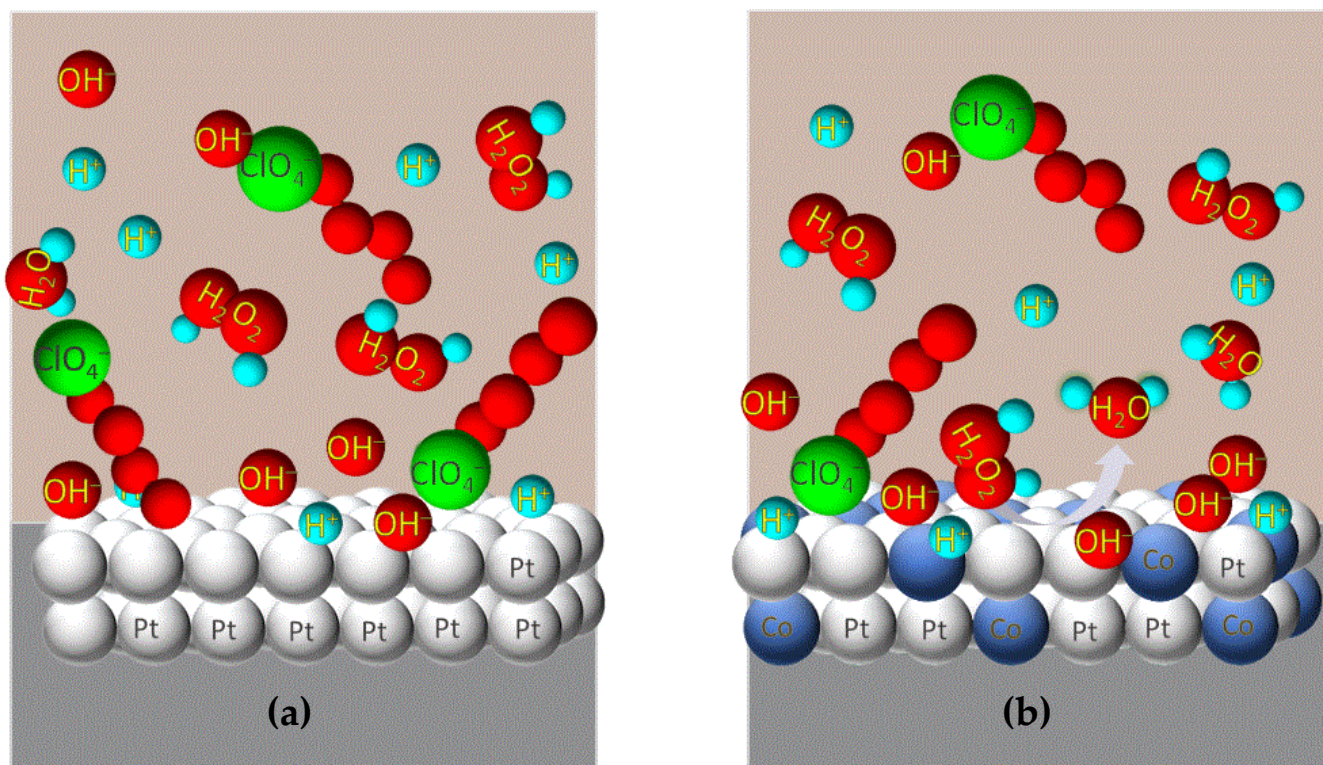


Figure 3. The catalysis of platinum on H_2O_2 reduction is constrained by the constant presence of adsorbed species on its surface (a). The presence of second metal in the electrode structure with the consequent alteration of the binding force of adsorbed species on the electrode surface results in a significant increase in active sites number for the catalysis of H_2O_2 cathodic reaction into H_2O (b).

The surface structure of the electrode also influences the susceptibility to ion adsorption on the Pt surface. Therefore, the electrode’s charge and the fraction of adsorbed anions concomitantly will influence the reactivity of Pt alloy single crystals on the electrode for the H_2O_2 reduction reaction. This way, the undesired adsorption of the anions from the electrolyte solution onto the platinum electrode surface will also contribute to the delay in the kinetics of the H_2O_2 cathodic reaction.

Similarly, the susceptibility to ion adsorption on the surface of platinum atoms is influenced by the change it undergoes due to the proximity of electrons from neighbouring atoms. The acquisition of different spatial arrangements leads to the distortion of the fcc unit cell structure of crystalline Pt on the electrode surface. Thus, the ensemble effect on the adsorption energy of H_2O_2 on the electrode surface is also evident by the Pt alloys exhibiting a change in the adsorption of unwanted anions from the electrolyte solution.

Therefore, the electrode's charge and the fraction of concurrently adsorbed anions will set Pt single crystals' reactivity along with the second metal at the electrode for the H_2O_2 reduction reaction.

Similarly, the occurrence of a less electronegative atom in the vicinity of platinum, such as copper [68,87], iron [75], nickel [18,87,90,91], cobalt [18], and palladium [74,92,93] will create an inductive effect on Pt local electron density, by reducing its d-band electrons' energy. Such an electronic properties shift reinforces the binding of the H_2O_2 and the intermediates OH_{ads} and H^+ on the catalyst surface, improving the catalytic action of the electrode surface towards H_2O_2 sensing.

Considering that metallic nanoparticles' support properties have an essential effect on the performance of the electrocatalysts used for the sensitive detection of H_2O_2 , the carbon-based material as a support is a good choice as it provides good conductivity and a high ECSA and can stabilise the nanoparticles. However, they must also have good corrosion resistance in the reaction medium, which is not always the case.

In aqueous solutions, carbon support materials may experience some corrosion problems, mainly when used as a cathode in the sensing devices, whenever the electrode potential goes up to 1.5 V vs. the reversible hydrogen electrode [98]. Such decomposition, catalysed by the presence of Pt nanoparticles deposited onto the carbon support, is responsible for the loss of carbon material that proceeds through the evolution of CO_2 , which acts as a passive species for the cathode reaction. This deterioration of the carbon is associated with the aggregation of the Pt catalyst nanoparticles on the carbon surface as corrosion intensifies, resulting in a decrease in ECSA and consequent fall in electrocatalytic performance and lifespan of the Pt nanoparticle-based electrode.

Therefore, one of the most promising approaches is incorporating more resistant supporting materials into the catalyst nanostructure, such as conductive metal oxides and conjugated conducting polymers.

Metal oxide nanoparticles are nanomaterials that exhibit intrinsic enzyme activity [99], referred to as "nanoenzymes." Though structurally different from natural enzymes (defined as three-dimensional structures of amino acid sequences), the crystal structures of metal oxide nanomaterials share certain similarities. These include their global size, shape, and surface charge, which allow them to mimic the action of natural enzymes. Indeed, iron oxide (Fe_3O_4) nanoparticles are one of the most typical nanozymes as they exhibit similar intrinsic enzymatic activity [100] to the biological horseradish peroxidase towards H_2O_2 reduction. Similarly, the high catalytic performance of cerium oxide (CeO_2) is well known [99]. This catalytic activity stems from the mixed-valence states of the redox pair Ce^{3+} and Ce^{4+} that can easily switch between each state in a cyclic process and from the presence of vacant oxygen sites that stabilise the Ce^{3+} oxidation state and make the oxygen lattice highly flexible. Likewise, cerium oxide nanoparticles exhibit a catalytic activity mimetic of several natural enzymes, including catalase which catalyses the breakdown of hydrogen peroxide into molecular oxygen and water. Accordingly, the concerted action of these nanoenzymes along with the platinum-based nanocomposites may explain the improved catalytic activity of the electrodes of Pt/ Fe_3O_4 /rGO [79], PtNi/ CeO_2 /NCNFs [91] hybrid films for the selective and sensitive detection of H_2O_2 .

Conductive mesoporous type polymers have potential applications as catalyst supports. Particularly polypyrrole (PPy) is a promising support material due to its good electrical conductivity and high stability in electrochemical processes [101]. In addition to providing higher catalyst stability when used as a support component for carbon-based and metal nanoparticles, PPy used as a support material for metal nanoparticles provides

an effective structure for the charge transfer on the electrode surface. It is expected that hybridised nanostructures of both conductive materials display a higher number of active sites and high electrical conductivity. Such hybridised nanostructure acts as high efficient co-catalysts (synergistic effect) in the H₂O₂ sensing [85,88].

4. Conclusions

The literature data reported in this review presented several proposals for coordinating Pt-based composites (in the form of alloys or single NPs) with other conductive materials, aiming to reduce the amount of platinum and simultaneously obtain a highly H₂O₂-sensitive transduction element. The literature surveys disclosed that catalysts of Pt-based alloys exhibit low working potential, fast electrochemical response, good reproducibility, and high sensitivity in the detection of H₂O₂.

The current study may provide a promising platform for non-enzymatic electrodes and affinity matrix assembly. The proposals presented for the alternative use of improved Pt-based alloy catalysts for the electro-reduction of H₂O₂ may be of practical interest for the assembly of sensors that can result in high-sensitive electrodes with lower Pt loadings.

Compared to the Pt-based catalyst, hybrid bimetallic catalysts often have a higher ECSA for electron transfer, which afford a higher catalytic activity. In addition, the increased free binding active sites of the Pt-based alloys electrocatalyst versus Pt have shown a higher ability to interact with the analyte, increasing the catalytic activity for H₂O₂ sensing. The hybrid electrocatalysts displayed good electrochemical performance for sensing H₂O₂ without any mediator or the addition of enzymes, showing a high peak current signal at a relatively low potential. The high performance of Pt-based bimetallic alloys for the sensing of H₂O₂ in a neutral media has also been observed. It is believed that these findings may guide the development of more efficient materials for highly sensitive electroanalysis of H₂O₂ for diagnostic purposes and therapeutic drug monitoring.

Author Contributions: Conceptualization, A.M. and P.R.; data curation, A.M.; writing—original draft preparation, A.M.; writing—review and editing, P.R., B.B. and M.N.; visualisation, A.M.; supervision, B.B. and M.N. All authors have read and agreed to the published version of the manuscript.

Funding: This project was financed by the Foundation for Science and Technology (FCT, Portugal) by grants UIDB/04567/2020 and UIDP/04567/2020. The work was supported by the PADDIC 2021-22 grant (A.M.) funded by ALIES—ASSOCIAÇÃO LUSÓFONA PARA O DESENVOLVIMENTO DA INVESTIGAÇÃO E ENSINO EM CIÊNCIAS DA SAÚDE.

Conflicts of Interest: The authors declare no conflict of interest.

References

1. Marzo, N.D.; Chisci, E.; Giovannoni, R. The Role of Hydrogen Peroxide in Redox-Dependent Signalling: Homeostatic and Pathological Responses in Mammalian Cells. *Cells* **2018**, *7*, 156. [[CrossRef](#)] [[PubMed](#)]
2. Pędziwiatr, P.; Mikołajczyk, F.; Zawadzki, D.; Mikołajczyk, K.; Bedka, A. Decomposition of hydrogen peroxide—kinetics and review of chosen catalysts. *Acta Innov.* **2018**, *26*, 45–52. [[CrossRef](#)]
3. Winterbourn, C. Biological Production, Detection and Fate of Hydrogen Peroxide. *Antioxid. Redox Signal.* **2017**, *29*, 541–551. [[CrossRef](#)] [[PubMed](#)]
4. Jin, A.H.; Li, B.S.; Dai, Z.J. Oxidative Desulfurization of Fuel Oil with Hydrogen Peroxide Catalyzed by Keggin-type Polyoxotungstate in a DC Magnetic Field. *Pet. Sci. Technol.* **2010**, *28*, 700–711. [[CrossRef](#)]
5. Li, L.; Lee, S.; Lae, H.L.; Youn, H.J. Hydrogen peroxide bleaching of hardwood kraft pulp with adsorbed birch xylan and its effect on paper properties. *BioResources* **2011**, *6*, 721–736. [[CrossRef](#)]
6. Hachem, C.; Bocquillon, F.; Zahraa, O.; Bouchy, M. Decolorization of textile industry wastewater by the photocatalytic degradation process. *Dye. Pigment.* **2001**, *49*, 117–125. [[CrossRef](#)]
7. Targhan, H.; Evans, P.; Bahrami, K. A review of the role of hydrogen peroxide in organic transformations. *J. Ind. Eng. Chem.* **2021**, *104*, 295–332. [[CrossRef](#)]
8. Pravda, J. Hydrogen peroxide and disease: Towards a unified system of pathogenesis and therapeutics. *Mol. Med.* **2020**, *26*, 41. [[CrossRef](#)]
9. Tredwin, C.J.; Naik, S.; Lewis, N.J.; Scully, C. Hydrogen peroxide tooth-whitening (bleaching) products: Review of adverse effects and safety issues. *Br. Dent. J.* **2006**, *200*, 371–376. [[CrossRef](#)]
10. Dutta, A.; Das, S.; Samanta, P.; Roy, S.; Adhikary, B.; Biswas, P. Non-enzymatic amperometric sensing of hydrogen peroxide at a CuS modified electrode for the determination of urine H₂O₂. *Electrochim. Acta* **2014**, *144*, 282–287. [[CrossRef](#)]

11. Ksibi, M. Chemical oxidation with hydrogen peroxide for domestic wastewater treatment. *Chem. Eng. J.* **2006**, *119*, 161–165. [[CrossRef](#)]
12. Anojčić, J.; Guzsivany, V.; Vajdle, O.; Kónya, Z.; Kalcher, K. Rapid amperometric determination of H₂O₂ by a Pt nanoparticle/Vulcan XC72 composite-coated carbon paste electrode in disinfection and contact lens solutions. *Monatsh. Chem.* **2018**, *149*, 1727–1738. [[CrossRef](#)]
13. Al-Attabi, Z.H.; D’Arcy, B.R.; Deeth, H.C. Effect of hydrogen peroxide on volatile sulphur compounds in UHT milk. In Proceedings of the Fifth Euro-Global Summit and Expo on Food & Beverages, Alicante, Spain, 16–18 June 2015.
14. Gerard, C.; Huguet, S.; Laurence, E.; Ferry, I.; Lafay, M.; Fouque, J.; Madar, O.; Rezai, K.; Giard, C. Permeability and Release of Decontaminating Agent Used in Cytotoxic Reconstitution Units: Diffusion of Hydrogen Peroxide in IV Bags. *Pharm. Technol. Hosp. Pharm.* **2017**, *2*, 17–21. [[CrossRef](#)]
15. Arefin, S.; Sarker, M.A.H.; Islam, M.A.; Harun-ur-Rashid, M.; Islam, M.N. Use of Hydrogen Peroxide (H₂O₂) in raw cow’s milk preservation. *J. Adv. Vet. Anim. Res.* **2017**, *4*, 371. [[CrossRef](#)]
16. Baharun, N.; Ling, O.P.; Ardani, M.R.; Ariffin, K.S.; Yaraghi, A.; Abdullah, N.S.; Putra, T.A.R.; Ismail, S. Effect of hydrogen peroxide and lead(II) nitrate on gold cyanide leaching of Malaysian mesothermal deposit gold ore. *Physicochem. Probl. Miner. Process.* **2020**, *56*, 905–918. [[CrossRef](#)]
17. Heravi, M.; Ghalavand, N.; Hashemi, E. Hydrogen Peroxide as a Green Oxidant for the Selective Catalytic Oxidation of Benzylic and Heterocyclic Alcohols in Different Media: An Overview. *Chemistry* **2020**, *2*, 101–178. [[CrossRef](#)]
18. Morais, A.; Salgado, J.R.; Sljukic, B.; Santos, D.; Sequeira, C. Electrochemical behaviour of carbon supported Pt electrocatalysts for H₂O₂ reduction. *Int. J. Hydrog. Energy* **2012**, *37*, 14143–14151. [[CrossRef](#)]
19. Daniel, G.; Zhang, Y.; Lanzalaco, S.; Brombin, F.; Kosmala, T.; Granozzi, G.; Wang, A.; Brillas, E.; Sirés, I.; Durante, C. Chitosan-Derived Nitrogen-Doped Carbon Electrocatalyst for a Sustainable Upgrade of Oxygen Reduction to Hydrogen Peroxide in UV-Assisted Electro-Fenton Water Treatment. *ACS Sustain. Chem. Eng.* **2020**, *8*, 14425–14440. [[CrossRef](#)]
20. Morais, A.L.; Rijo, P.; Batanero Hernán, M.B.; Nicolai, M. Biomolecules and Electrochemical Tools in Chronic Non-Communicable Disease Surveillance: A Systematic Review. *Biosensors* **2020**, *10*, 121. [[CrossRef](#)]
21. Hernandez, K.; Berenguer-Murcia, A.; Rodrigues, R.C.; Fernandez-Lafuente, R. Hydrogen Peroxide in Biocatalysis. A Dangerous Liaison. *Curr. Org. Chem.* **2012**, *16*, 2652–2672. [[CrossRef](#)]
22. Liang, F.; Hu, L.; Li, Y.; Majeed, S.; Li, H.; Cai, H.; Yang, X.; Xu, G. Low-potential determination of hydrogen peroxide, uric acid and uricase based on highly selective oxidation of p-hydroxyphenylboronic acid by hydrogen peroxide. *Sens. Actuators B Chem.* **2013**, *178*, 144–148. [[CrossRef](#)]
23. Bienert, G.P.; Chaumont, F. Aquaporin-facilitated transmembrane diffusion of hydrogen peroxide. *Biochim. Biophys. Acta* **2014**, *1840*, 1596–1604. [[CrossRef](#)] [[PubMed](#)]
24. Kehrer, J.P.; Koltz, L. Free radicals and related reactive species as mediators of tissue injury and disease: Implications for Health. *Crit. Rev. Toxicol.* **2015**, *45*, 765–798. [[CrossRef](#)] [[PubMed](#)]
25. Molavian, H.; Tonekaboni, A.M.; Kohandel, M.; Sivaloganathan, S. The Synergetic Coupling among the Cellular Antioxidants Glutathione Peroxidase/Peroxiredoxin & Other Antioxidants and its Effect on the Concentration of H₂O₂. *Sci. Rep.* **2015**, *5*, 13620. [[CrossRef](#)]
26. Lennicke, C.; Rahn, J.; Lichtenfels, R.; Wessjohann, L.A.; Seliger, B. Hydrogen peroxide—production, fate and role in redox signaling of tumor cells. *Cell Commun. Signal* **2015**, *13*, 39. [[CrossRef](#)]
27. Steven, S.; Frenis, K.; Oelze, M.; Kalinovic, S.; Kuntic, M.; Bayo Jimenez, M.T.; Vujacic-Mirski, K.; Helmstädter, J.; Kröller-Schön, S.; Münzel, T.; et al. Vascular Inflammation and Oxidative Stress: Major Triggers for Cardiovascular Disease. *Oxid. Med. Cell Longev.* **2019**, *2019*, 7092151. [[CrossRef](#)]
28. Dimozi, A.; Mavrogonatou, E.; Sklirou, A.; Kleatsas, D. Oxidative stress inhibits the proliferation, induces premature senescence and promotes a catabolic phenotype in human nucleus pulposus intervertebral disc cells. *Eur. Cells Mater.* **2015**, *30*, 89–103. [[CrossRef](#)]
29. Li, J.; Li, W.; Su, J.; Liu, W.; Altura, B.T.; Altura, B.M. Hydrogen peroxide induces apoptosis in cerebral vascular smooth muscle cells: Possible relation to neurodegenerative diseases and strokes. *Brain Res. Bull.* **2003**, *62*, 101–106. [[CrossRef](#)]
30. Biswas, S.K. Does the Interdependence between Oxidative Stress and Inflammation Explain the Antioxidant Paradox? *Oxid. Med. Cell Longev.* **2016**, *2016*, 5698931. [[CrossRef](#)]
31. Ratliff, B.B.; Abdulmahdi, W.; Pawar, R.; Wolin, M.S. Oxidant Mechanisms in Renal Injury and Disease. *Antioxid. Redox Signal.* **2016**, *25*, 119–146. [[CrossRef](#)]
32. Zhang, J.; Wang, X.; Vikash, V.; Ye, Q.; Wu, D.; Liu, Y.; Dong, W. ROS and ROS-Mediated Cellular Signalling. *Oxid. Med. Cell Longev.* **2016**, *2016*, 4350965. [[CrossRef](#)] [[PubMed](#)]
33. Runchel, C.; Matsuzawa, A.; Ichijo, H. Mitogen-activated protein kinases in mammalian oxidative stress responses. *Antioxid. Redox Signal* **2011**, *15*, 205–218. [[CrossRef](#)]
34. Tabner, B.J.; Turnbull, S.; Fullwood, N.J.; German, M.; Allsop, D. The production of hydrogen peroxide during early-stage protein aggregation: A common pathological mechanism in different neurodegenerative diseases? *Biochem. Soc. Trans.* **2005**, *33*, 548–550. [[CrossRef](#)]
35. Zhao, J.; Yan, Y.; Zhu, L.; Li, X.; Li, G. An amperometric biosensor for the detection of hydrogen peroxide released from human breast cancer cells. *Biosens. Bioelectron.* **2013**, *41*, 815–819. [[CrossRef](#)] [[PubMed](#)]
36. Steinhorn, B.; Sorrentino, A.; Badole, S.; Bogdanova, Y.; Belousov, V.; Michel, T. Chemogenetic generation of hydrogen peroxide in the heart induces severe cardiac dysfunction. *Nat. Commun.* **2018**, *9*, 4044. [[CrossRef](#)] [[PubMed](#)]

37. Oh, W.-K.; Jeong, Y.S.; Kim, S.; Jang, J. Fluorescent polymer nanoparticle for selective sensing of intracellular hydrogen peroxide. *ACS Nano* **2012**, *6*, 8516–8524. [CrossRef]
38. Magara, K.; Ikeda, T.; Sugimoto, T.; Hosoya, S. Quantitative Analysis of Hydrogen Peroxide by High Performance Liquid Chromatography. *Japan Tappi J.* **2007**, *61*, 1481–1493. [CrossRef]
39. Tahirović, A.; Copra, A.; Omanović-Miklicanin, E.; Kalcher, K. A chemiluminescence sensor for the determination of hydrogen peroxide. *Talanta* **2007**, *72*, 1378–1385. [CrossRef]
40. Gimeno, M.; Mayoral, M.; Andrés, J. A potentiometric titration for H₂O₂ determination in the presence of organic compounds. *Anal. Methods* **2013**, *5*, 1510–1514. [CrossRef]
41. Dhara, K.; Mahapatra, D.R. Recent advances in electrochemical nonenzymatic hydrogen peroxide sensors based on nanomaterials: A review. *J. Mater. Sci.* **2019**, *54*, 12319–12357. [CrossRef]
42. Ledo, A.; Fernandes, E.; Brett, C.; Barbosa, R. Enhanced Selectivity and Stability of Ruthenium Purple-Modified Carbon Fiber Microelectrodes for Detection of Hydrogen Peroxide in Brain Tissue. *Sens. Actuators B Chem.* **2020**, *311*, 127899. [CrossRef]
43. Chaisuksant, R.; Chomsook, T.; Manthong, N.; Kalcher, K. Low Cost Hydrogen Peroxide Sensor from Manganese Oxides Modified Pencil Graphite Electrode. *Procedia Chem.* **2016**, *20*, 81–84. [CrossRef]
44. Katsounaros, I.; Schneider, W.B.; Meier, J.; Benedikt, U.; Biedermann, P.U.; Auer, A.A.; Mayrhofer, K.J.J. Hydrogen peroxide electrochemistry on platinum: Towards understanding the oxygen reduction reaction mechanism. *Phys. Chem. Chem. Phys.* **2012**, *14*, 7384–7391. [CrossRef]
45. Elewi, A.; AL-Shammaree, S.; Al-sammarraie, A. Hydrogen peroxide biosensor based on hemoglobin-modified gold nanoparticles–screen printed carbon electrode. *Sens. Bio-Sens. Res.* **2020**, *28*, 100340. [CrossRef]
46. Chen, J.; Yu, Q.; Fu, W.; Chen, X.; Zhang, Q.; Dong, S.; Chen, H.; Zhang, S. A Highly Sensitive Amperometric Glutamate Oxidase Microbiosensor Based on a Reduced Graphene Oxide/Prussian Blue Nanocube/Gold Nanoparticle Composite Film-Modified Pt Electrode. *Sensors* **2020**, *20*, 2924. [CrossRef]
47. Si, B.; Song, E. Recent Advances in the Detection of Neurotransmitters. *Chemosensors* **2018**, *6*, 1. [CrossRef]
48. Sanford, A.L.; Morton, S.W.; Whitehouse, K.L.; Oara, H.M.; Lugo-Morales, L.Z.; Roberts, J.G.; Sombers, L.A. Voltammetric Detection of Hydrogen Peroxide at Carbon Fiber Microelectrodes. *Anal. Chem.* **2010**, *82*, 5205–5210. [CrossRef]
49. Pullano, S.A.; Greco, M.; Bianco, M.G.; Foti, D.; Brunetti, A.; Fiorillo, A.S. Glucose biosensors in clinical practice: Principles, limits and perspectives of currently used devices. *Theranostics* **2022**, *12*, 493–511. Available online: <https://www.thno.org/v12p0493.htm> (accessed on 15 March 2022). [CrossRef]
50. Homaei, A.A.; Sariri, R.; Vianello, F.; Stevanato, R. Enzyme immobilization: An update. *J. Chem. Biol.* **2013**, *6*, 185–205. [CrossRef]
51. Swamy, N.K.; Sandeep, S.; Santhosh, A.S. Enzyme Immobilization Methods and Role of Conductive Polymers in Fabrication of Enzymatic Biosensors. *Indian J. Adv. Chem. Sci.* **2017**, *S2*, 1–5. [CrossRef]
52. Sin, M.L.; Mach, K.E.; Wong, P.K.; Liao, J.C. Advances and challenges in biosensor-based diagnosis of infectious diseases. *Expert Rev. Mol. Diagn.* **2014**, *14*, 225–244. [CrossRef] [PubMed]
53. Zhu, H.; Li, L.; Zhou, W.; Shao, Z.; Chen, X. Advances in Non-Enzymatic Glucose Biosensors Based on Metal Oxides. *J. Mater. Chem. B* **2016**, *4*, 7333–7349. [CrossRef] [PubMed]
54. Defnet, P.A.; Han, C.; Zhang, B. Temporally-Resolved Ultrafast Hydrogen Adsorption and Evolution on Single Platinum Nanoparticles. *Anal. Chem.* **2019**, *91*, 4023–4030. [CrossRef] [PubMed]
55. Ramachandran, R.; Chen, S.-M.; Thangaraj, B.; Elumalai, P.; Raja, P.; Chen, T.-W.; Kannan, R.; Kannaiyan, D.; George, G. A review of the advanced developments of electrochemical sensors for the detection of toxic and bioactive molecules. *Inorg. Chem. Front.* **2019**, *6*, 3418–3439. [CrossRef]
56. Rai, M.; Gade, A.; Gaikwad, S.; Marcato, P.D.; Durán, N. Biomedical Applications of Nanobiosensors: The State-of-the-Art. *J. Braz. Chem. Soc.* **2012**, *23*, 14–24. [CrossRef]
57. Wang, M.; Feng, B.; Li, H.; Li, H. Controlled Assembly of Hierarchical Metal Catalysts with Enhanced Performances. *Cell* **2019**, *5*, 805–837. [CrossRef]
58. Prasai, B.; Wilson, A.; Wiley, B.J.; Ren, Y.; Petkov, V. On the road to metallic nanoparticles by rational design: Bridging the gap between atomic-level theoretical modeling and reality by total scattering experiments. *Nanoscale* **2015**, *7*, 17902–17922. [CrossRef]
59. Gomez, C.G.; Silva, A.M.; Strumia, M.C.; Avalle, L.B.; Rojas, M.I. The origin of high electrocatalytic activity of hydrogen peroxide reduction reaction by a g-C₃N₄/HOPG sensor. *Nanoscale* **2017**, *9*, 11170–11179. [CrossRef]
60. Welch, C.M.; Compton, R.G. The use of nanoparticles in electroanalysis: A review. *Anal. Bioanal. Chem.* **2006**, *384*, 601–619. [CrossRef]
61. Yang, G.; Akhade, S.; Chen, X.; Liu, Y.; Lee, M.-S.; Glezakou, V.-A.; Rousseau, R.; Lercher, J. Nature of Hydrogen Adsorption on Platinum in the Aqueous Phase. *Angew. Chem. Int. Ed.* **2018**, *58*, 3527–3532. [CrossRef]
62. Rodriguez, J.A.; Goodman, D.W. Dissociative adsorption and hydrogenolysis of ethane over clean and nickel-covered platinum (111). *J. Phys. Chem.* **1990**, *94*, 5342–5347. [CrossRef]
63. Li, K.; Yan, S.; Chen, H.; Wang, B.; Li, G.; Shi, Y.; Xu, X. Facile Solvothermal Synthesis of Hybrid SnS₂/Platinum Nanoparticles for Hydrogen Peroxide Biosensing. *J. Bionanosci.* **2015**, *9*, 335–340. [CrossRef]
64. Chen, W.; Cao, J.; Fu, W.; Zhang, J.; Qian, G.; Yang, J.; Chen, D.; Zhou, X.; Yuan, W.; Duan, X. Molecular-Level Insights into the Notorious CO Poisoning of Platinum Catalyst. *Angew. Chem. (Int. Ed. Engl.)* **2022**, *61*, e202200190. [CrossRef] [PubMed]
65. Molochas, C.; Tsiakaras, P. Carbon Monoxide Tolerant Pt-Based Electrocatalysts for H₂-PEMFC Applications: Current Progress and Challenges. *Catalysts* **2021**, *11*, 1127. [CrossRef]

66. Al-Akraa, I. A Simple and Effective Way to Overcome Carbon Monoxide Poisoning of Platinum Surfaces in Direct Formic Acid Fuel Cells. *Int. J. Electrochem. Sci.* **2019**, *14*, 8267–8275. [[CrossRef](#)]
67. Valdés-López, V.; Mason, T.; Shearing, P.; Brett, D.J.L. Carbon monoxide poisoning and mitigation strategies for polymer electrolyte membrane fuel cells—A review. *Prog. Energy Combust. Sci.* **2020**, *79*, 100842. [[CrossRef](#)]
68. Zhao, W.; Jin, J.; Wu, H.; Wang, S.; Fneg, C.; Yang, S.; Ding, Y. Electrochemical hydrogen peroxide sensor based on carbon supported Cu@Pt core-shell nanoparticles. *Mater. Sci. Eng. C Mater. Biol. Appl.* **2017**, *78*, 185–190. [[CrossRef](#)]
69. Yu, G.; Wu, W.; Pan, X.; Zhao, Q.; Wei, X.; Lu, Q. High Sensitive and Selective Sensing of Hydrogen Peroxide Released from Pheochromocytoma Cells Based on Pt-Au Bimetallic Nanoparticles Electrodeposited on Reduced Graphene Sheets. *Sensors* **2015**, *15*, 2709–2722. [[CrossRef](#)]
70. Gu, Y.; Chen, C.C. Eliminating the Interference of Oxygen for Sensing Hydrogen Peroxide with the Polyaniline Modified Electrode. *Sensors* **2008**, *8*, 8237–8247. [[CrossRef](#)]
71. Mueller, J.E.; Krttil, P.; Kibler, L.A.; Jacob, T. Bimetallic alloys in action: Dynamic atomistic motifs for electrochemistry and catalysis. *Phys. Chem. Chem. Phys.* **2014**, *16*, 15029–15042. [[CrossRef](#)]
72. Yang, Z.; Nakashima, N. A simple preparation of very high methanol tolerant cathode electrocatalyst for direct methanol fuel cell based on polymer-coated carbon nanotube/platinum. *Sci. Rep.* **2015**, *5*, 12236–12245. [[CrossRef](#)] [[PubMed](#)]
73. Rick, J.; Tsai, M.-C.; Hwang, B.J. Biosensors Incorporating Bimetallic Nanoparticles. *Nanomaterials* **2016**, *6*, 5. [[CrossRef](#)] [[PubMed](#)]
74. Niu, X.; Chen, C.; Zhao, H.; Chai, Y.; Lan, M. Novel snowflake-like Pt-Pd bimetallic clusters on screen-printed gold nanofilm electrode for H₂O₂ and glucose sensing. *Biosens. Bioelectron.* **2012**, *36*, 262–266. [[CrossRef](#)]
75. Mei, H.; Wu, W.; Yu, B.; Wu, H.; Wang, S.; Xia, Q.-H. Nonenzymatic electrochemical sensor based on Fe@Pt core-shell nanoparticles for hydrogen peroxide, glucose and formaldehyde. *Sens. Actuators B Chem.* **2016**, *223*, 68–75. [[CrossRef](#)]
76. Wang, T.; Pan, L.; Zhang, X.; Zou, J.-J. Insights into the Pt (111) Surface Aid in Predicting the Selective Hydrogenation Catalyst. *Catalysts*. **2020**, *10*, 1473. [[CrossRef](#)]
77. Xin, H.; Linic, S. Communications: Exceptions to the d-band model of chemisorption on metal surfaces: The dominant role of repulsion between adsorbate states and metal d-states. *J. Chem. Phys.* **2010**, *132*, 221101. [[CrossRef](#)]
78. Oliveira-Brett, A.M. Electron Transfer Reactions in Biological Systems. In *Chemistry, Molecular Sciences and Chemical Engineering*; Elsevier: Amsterdam, The Netherlands, 2017; pp. 1–8. [[CrossRef](#)]
79. Zhao, X.; Li, Z.; Chen, C.; Wu, Y.; Zhu, Z.; Zhao, H.; Lan, M. A Novel Biomimetic Hydrogen Peroxide Biosensor Based on Pt Flowers-decorated Fe₃O₄/Graphene Nanocomposite. *Electroanalysis* **2017**, *29*, 1518–1523. [[CrossRef](#)]
80. Tajabadi, M.T.; Sookhakian, M.; Zalnezhad, E.; Yoon, G.H.; Hamouda, A.M.S.; Azarang, M.; Basirun, W.J.; Alias, Y. Electrodeposition of flower-like platinum on electrophoretically grown nitrogen-doped graphene as a highly sensitive electrochemical non-enzymatic biosensor for hydrogen peroxide detection. *Appl. Surf. Sci.* **2016**, *386*, 418–426. [[CrossRef](#)]
81. Detsi, E.; Tolbert, S.; Punzhin, S.; De Hosson, J.T.M. Metallic muscles and beyond: Nanofoams at work. *J. Mater. Sci.* **2015**, *51*, 615–634. [[CrossRef](#)]
82. Guo, S.; Li, J.; Ren, W.; Wen, D.; Dong, S.; Wang, E. Carbon Nanotube/Silica Coaxial Nanocable as a Three-Dimensional Support for Loading Diverse Ultra-High-Density Metal Nanostructures: Facile Preparation and Use as Enhanced Materials for Electrochemical Devices and SERS. *Chem. Mater.* **2009**, *21*, 2247–2257. [[CrossRef](#)]
83. Thirumalraj, B.; Sakthivel, R.; Chen, S.-M.; Rajkumar, C.; Yu, L.-k.; Kubendhiran, S. A reliable electrochemical sensor for determination of H₂O₂ in biological samples using platinum nanoparticles supported graphite/gelatin hydrogel. *Microchem. J.* **2019**, *146*, 673–678. [[CrossRef](#)]
84. Lakard, B. Electrochemical Biosensors Based on Conducting Polymers: A Review. *Appl. Sci.* **2020**, *10*, 6614. [[CrossRef](#)]
85. Oliveira, R.C.P.; Milikić, J.; Daş, E.; Yurtcan, A.B.; Santos, D.M.F.; Šljukić, B. Platinum/polypyrrole-carbon electrocatalysts for direct borohydride-peroxide fuel cells. *Appl. Catal. B Environ.* **2018**, *238*, 454–464. [[CrossRef](#)]
86. Xing, L.; Rong, Q.; Ma, Z. Non-enzymatic electrochemical sensing of hydrogen peroxide based on polypyrrole/platinum nanocomposites. *Sens. Actuators B Chem.* **2015**, *221*, 242–247. [[CrossRef](#)]
87. Mei, H.; Wu, H.; Wu, W.; Wang, S.; Xia, Q. Ultrasensitive electrochemical assay of hydrogen peroxide and glucose based on PtNi alloy decorated MWCNTs. *RSC Adv.* **2015**, *5*, 102877–102884. [[CrossRef](#)]
88. Gutierrez, F.A.; Giordana, I.S.; Fuertes, V.C.; Montemerlo, A.E.; Sieben, J.M.; Alvarez, A.E.; Rubianes, M.D.; Rivas, G.A. Analytical applications of Cu@PtPd/C nanoparticles for the quantification of hydrogen peroxide. *Microchem. J.* **2018**, *141*, 240–246. [[CrossRef](#)]
89. Cardoso, D.S.P.; Santos, D.M.F.; Šljukić, B.; Sequeira, C.A.C.; Macciò, D.; Saccone, A. Platinum-rare earth cathodes for direct borohydride-peroxide fuel cells. *J. Power Sources* **2016**, *307*, 251–258. [[CrossRef](#)]
90. Guan, H.; Zhao, Y.; Zhang, J.; Liu, Y.; Yuan, S.; Zhang, B. Uniformly dispersed PtNi alloy nanoparticles in porous N-doped carbon nanofibers with high selectivity and stability for hydrogen peroxide detection. *Sens. Actuators B Chem.* **2018**, *261*, 354–363. [[CrossRef](#)]
91. Guan, H.; Zhao, Y.; Zhang, J.; Liu, Y.; Zhang, B. Rapid quantitative determination of hydrogen peroxide using an electrochemical sensor based on PtNi alloy/CeO₂ plates embedded in N-doped carbon nanofibers. *Electrochim. Acta* **2018**, *295*, 997–1005. [[CrossRef](#)]
92. Yang, H.; Wang, Z.; Zhou, Q.; Xu, C.; Hou, J. Nanoporous platinum-copper flowers for non-enzymatic sensitive detection of hydrogen peroxide and glucose at near-neutral pH values. *Mikrochim. Acta* **2019**, *186*, 631. [[CrossRef](#)]
93. Li, H.; Zhao, H.; He, H.; Shi, L.; Cai, X.; Lan, M. Pt-Pd bimetallic nanocoral modified carbon fiber microelectrode as a sensitive hydrogen peroxide sensor for cellular detection. *Sens. Actuators B Chem.* **2018**, *260*, 174–182. [[CrossRef](#)]

94. Darby, M.T.; Sykes, E.C.H.; Michaelides, A.; Stamatakis, M. Carbon Monoxide Poisoning Resistance and Structural Stability of Single Atom Alloys. *Top. Catal.* **2018**, *61*, 428–438. [[CrossRef](#)] [[PubMed](#)]
95. Statista Market and Consumption Website Data Homepage. Available online: <https://www.statista.com/> (accessed on 23 March 2022).
96. Zhang, Z.-P.; Zhang, Y.-W.; Jiang, H. Fundamentals and Structural Characterization of Shape-Controlled Bimetallic Nanostructures. In *Bimetallic Nanostructures-Shape-Controlled Synthesis for Catalysis, Plasmonics, and Sensing Applications*; Zhang, Y.-W., Ed.; John Wiley & Sons, Inc.: Hoboken, NJ, USA, 2018; pp. 3–51.
97. Katsounaros, I.; Schneider, W.B.; Meier, J.C.; Benedikt, U.; Biedermann, P.U.; Auer, A.A.; Cuesta, A.; Mayrhofer, K.J.J. The impact of spectator species on the interaction of H₂O₂ with platinum—implications for the oxygen reduction reaction pathways. *Phys. Chem. Chem. Phys.* **2013**, *15*, 8058–8068. [[CrossRef](#)] [[PubMed](#)]
98. Castanheira, L.F.; Dubau, L.; Mermoux, M.; Berthomé, G.; Caque, N.; Rossinot, E.; Chatenet, M.; Maillard, F. Carbon Corrosion in Proton-Exchange Membrane Fuel Cells: From Model Experiments to Real-Life Operation in Membrane Electrode Assemblies. *ACS Catal.* **2014**, *4*, 2258–2267. [[CrossRef](#)]
99. Wang, X.; Guo, W.; Hu, Y.; Wu, J.; Wei, H. Metal Oxide-Based Nanomaterials for Nanozymes. In *Nanozymes: Next Wave of Artificial Enzymes*; Wang, X., Guo, W., Hu, Y., Wu, J., Wei, H., Eds.; Springer: Berlin/Heidelberg, Germany, 2016; pp. 57–91.
100. Gao, L.Z.; Zhuang, J.; Nie, L.; Zhang, J.B.; Zhang, Y.; Gu, N.; Wang, T.H.; Feng, J.; Yang, D.L.; Perrett, S.; et al. Intrinsic peroxidase-like activity of ferromagnetic nanoparticles. *Nat. Nanotechnol.* **2007**, *2*, 577–583. [[CrossRef](#)]
101. Zhou, Q.; Shi, G. Conducting Polymer-Based Catalysts. *J. Am. Chem. Soc.* **2016**, *138*, 2868–2876. [[CrossRef](#)]